Marat Yuldashev

Mathematical Models and Simulation of Costas Loops

JYVÄSKYLÄN YLIOPISTO

Marat Yuldashev

Mathematical Models and Simulation of Costas Loops

UNIVERSITY OF JYVÄSKYLÄ

JYVÄSKYLÄ 2013

Mathematical Models and Simulation of Costas Loops

Marat Yuldashev

Mathematical Models and Simulation of Costas Loops

ABSTRACT

This work is devoted to the development of nonlinear mathematical models of Costas loops. A Costas loop was invented in 1956 by John P. Costas of General Electric. Nowadays, a Costas loop is widely used in many applications including telecommunication devices, global positioning systems (GPS), medical implants, mobile phones, and other gadgets.

Costas loop is a phase-locked loop (PLL) based circuit designed to simultaneously perform two tasks — carrier recovery and data demodulation. To performs both of these tasks it has three non-linear elements. So, Costas loop is more complicated circuit than analog PLLs with only one nonlinear element and therefore requires special techniques for its analysis. All this makes the development of non-linear models of Costas loops a difficult task. For high-frequency signals, used in the modern devices, the transient time is thousands of times greater than the signal's periods. This property of Costas loop further complicates the application of analytical methods and numerical simulation. Also the signal waveforms involved greatly affect the behaviour of Costas circuits.

In this work, nonlinear mathematical models of the BPSK Costas loop and the Quadrature Phase Shift Keying (QPSK) Costas loop have been developed. These models allow to facilitate the application of analytical methods and reduce the numerical simulation time, which is a practically relevant significant problem. All theoretical results are rigorously proved. An effective numerical procedure for the simulation of Costas loops based on the phase-detector characteristics is proposed.

Keywords: Costas loop, carrier tracking, GPS, PLL, BPSK, QPSK Costas

Author   Marat Yuldashev
                        Department of Mathematical Information Technology
                        University of Jyväskylä, Finland

                        Faculty of Mathematics and Mechanics
                        Saint-Petersburg State University, Russia

Supervisors   Docent Nikolay Kuznetsov
                        Department of Mathematical Information Technology
                        University of Jyväskylä, Finland

                        Professor Gennady A. Leonov
                        Faculty of Mathematics and Mechanics
                        Saint Petersburg State University, Russia

                        Professor Pekka Neittaanmäki
                        Department of Mathematical Information Technology
                        University of Jyväskylä, Finland

                        Professor Timo Tiihonen
                        Department of Mathematical Information Technology
                        University of Jyväskylä, Finland

Reviewers   Professor Sergei Abramovich
                        School of Education and Professional Studies
                        State University of New York at Potsdam, USA

                        Professor Ivan Zelinka
                        Department of Computer Science
                        VŠB-TUO, Czech Republic

Opponent   Professor Vladimir Rasvan
                        Faculty of Automatics, Computers
                        and Electronics
                        University of Craiova, Romania

ACKNOWLEDGEMENTS

LIST OF FIGURES

LIST OF TABLES

CONTENTS

LIST OF INCLUDED ARTICLES

PI   Best R.E.,Kuznetsov N.V.,Leonov G.A., Yuldashev M.V.,Yuldashev R.V.. Nonlinear Analysis of Phase-Locked Loop Based Circuits. *Discontinuity and Complexity in Nonlinear Physical Systems (eds. J.T. Machado, D. Baleanu, A. Luo), Springer, ISBN 978-3-319-01410-4*, 2014.

PII   Kuznetsov N.V., Leonov G.A., Neittaanmäki P., Seledzhi S.M., Yuldashev M.V.,Yuldashev R.V.. Nonlinear Analysis of Costas Loop Circuit. *ICINCO 2013 - Proceedings of the 9th International Conference on Informatics in Control, Automation and Robotics, pp.427–433*, 2013.

PIII   Kuznetsov N.V., Leonov G.A., Neittaanmäki P., Yuldashev M.V.,Yuldashev R.V.. Nonlinear Mathematical Models of Costas Loop for General Waveform of Input Signal. *IEEE 4th International Conference on Nonlinear Science and Complexity, NSC 2012 - Proceedings, pp. 75–80*, 2012.

PIV   Leonov G.A., Kuznetsov N.V.,Yuldashev R.V.,Yuldashev M.V.. Differential Equations of Costas Loop. *Doklady Mathematics, Vol. 86, No. 2, pp. 723–728*, 2012.

PV   Kuznetsov N.V.,Leonov G.A., Yuldashev M.V.,Yuldashev R.V.. Nonlinear Analysis of Costas Loop Circuit. *ICINCO 2012 - Proceedings of the 9th International Conference on Informatics in Control, Automation and Robotics, Vol. 1, pp. 557–560*, 2012.

PVI   Leonov G.A., Kuznetsov N.V., Yuldashev M.V., Yuldashev R.V.. Analytical Method for Computation of Phase-Detector Characteristic. *IEEE Transactions On Circuits And Systems-II: Express Briefs, Vol. 59, Iss. 10, pp. 633–637*, 2012.

OTHER PUBLICATIONS

AI N. V. Kuznetsov, G. A. Leonov, S.M. Seledzhi, M. V. Yuldashev, R. V. Yuldashev. Nonlinear Analysis of Phase-Locked Loop with Squarer. *IFAC Proceedings Volumes (IFAC-PapersOnline) (5th IFAC International Workshop on Periodic Control Systems, Caen, France) 2013, Vol. 5, pp. 80-85, 2013.*

AII N. V. Kuznetsov, G. A. Leonov, M. V. Yuldashev, R. V. Yuldashev. Phase Synchronization in Analog and Digital Circuits. *Plenary lecture, SPb:5-aya rossijskaya Mul'tiKonferentsiya po Problemam Upravleniya,* pp. 24–31, 2012.

AIII N. V. Kuznetsov, G. A. Leonov, M. V. Yuldashev, R. V. Yuldashev. Nonlinear Analysis of Analog Phase-Locked Loop. *Proceedings of International conference Dynamical Systems and Applications,* pp. 21–22, 2012.

AIV N. V. Kuznetsov, G. A. Leonov, P. Neittaanmäki, S. M. Seledzhi, M. V. Yuldashev, R. V. Yuldashev. Simulation of Phase-Locked Loops in Phase-Frequency Domain. *IEEE International Congress on Ultra Modern Telecommunications and Control Systems and Workshops,* pp. 351–356, 2012.

AV M.V. Yuldashev. Nonlinear analysis of Costas loop. *XII International Workshop "Stability and Oscillations of Nonlinear Control Systems",* pp. 348–350, 2012.

AVI M.V. Yuldashev. Nonlinear Analysis of BPSK Device. *Proceedings of the 3rd Inter-University Conference on Informatics*, pp. 457–458, 2012 [in Russian].

AVII G. A. Leonov, N. V. Kuznetsov, M. V. Yuldashev, R. V. Yuldashev. Computation of Phase Detector Characteristics in Synchronization Systems. *Doklady Mathematics*, Vol. 84, No. 1, pp. 586–590, 2011.

AVIII N. V. Kuznetsov, G. A. Leonov, M. V. Yuldashev, R. V. Yuldashev. Analytical methods for computation of phase-detector characteristics and PLL design. *International Symposium on Signals, Circuits and Systems*, pp. 1–4, IEEE press, 2011.

AIX N. V. Kuznetsov, G. A. Leonov, P. Neittaanmäki, S. M. Seledzhi, M. V. Yuldashev, R. V. Yuldashev. High-frequency analysis of phase-locked loop and phase detector characteristic computation. *8th International Conference on Informatics in Control, Automation and Robotics (ICINCO 2011)*, Vol. 1, pp. 272–278, INSTICC Press, 2011.

AX M.V. Yuldashev. Phase Detector Characteristics Computation for Two Impulse Signals. *Proceedings of the 2nd Inter-University Conference on Informatics*, pp. 389–390, 2011 [in Russian].

AXI N. V. Kuznetsov, G. A. Leonov, P. Neittaanmäki, S. M. Seledzhi, M. V. Yuldashev, R. V. Yuldashev. Nonlinear Analysis of Phase-locked loop. *IFAC Proceedings Volumes (IFAC-PapersOnline)*, Vol. 4, No. 1, pp. 34–38, 2010.

PATENTS

AXII N. V. Kuznetsov, G. A. Leonov, P. Neittaanmäki, M. V. Yuldashev, R. V. Yul-dashev. *Patent application.* Method And System For Modeling Costas Loop Feedback For Fast Mixed Signals Solutions. FI 20130124, 2013.

AXIII N. V. Kuznetsov, G. A. Leonov, S. M. Seledzhi, M. V. Yuldashev, R. V. Yul-dashev. Patent. Modulator of Phase Detector Parameters. RU 2449463 C1, 2011.

AXIV N. V. Kuznetsov, G. A. Leonov, S. M. Seledzhi, M. V. Yuldashev, R. V. Yul-dashev. Patent. The Method and Device for Determining of Characteristics of Phase-Locked Loop Generators. RU 11255 U1, 2011.

AXV N. V. Kuznetsov, G. A. Leonov, S. M. Seledzhi, M. V. Yuldashev, R. V. Yulda-shev. Patent on software. Program for Determining and Simulation of the Main Characteristics of Phase-Locked Loops (MR). RU 2011613388, 2011.

AXVI N. V. Kuznetsov, G. A. Leonov, S. M. Seledzhi, M. V. Yuldashev, R. V. Yulda-shev. Patent on software. Program for Determining and Simulation of the Main Characteristics of Costas Loops (CLMod). RU 2011616770, 2011.

1 INTRODUCTION AND THE STRUCTURE OF THE WORK

1.1 Introduction

The Costas loop was proposed by American engineer John Costas of General Electric (Costas, 1956, 1962) in 1956. A Costas loop is a Binary Phase Shift Keying (BPSK) data recovery and carrier tracking circuit (Tomasi, 2001; Young, 2004; Couch, 2007; Proakis and Salehi, 2007; Best, 2007; Chen et al., 2010). Nowadays, various modifications of Costas loop are widely used in Global Positioning Systems (GPS) (Mileant and Hinedi, 1994; Tang et al., 2010; Braasch and Van Dierendonck, 1999; Tanaka et al., 2001; Humphreys et al., 2005; An'an and Du Yong, 2006; Kaplan and Hegarty, 2006; Misra and Palod, 2011; Hegarty, 2012; Jasper, 1987; Beier, 1987), telecommunication devices (Viterbi, 1983; Malyon, 1984; Hodgkinson, 1986; Stephens, 2001; Yu et al., 2011; Abe et al., 2012), medical systems (Iniewski, 2008; Hu and Sawan, 2005; Luo and Sonkusale, 2008; Xu et al., 2009), mobile phones (Kobayashi et al., 1992; Gao and Feher, 1996; Lin et al., 2004; Shah and Sinha, 2009), and other important technological applications (Wang and Leeb, 1987; Miyazaki et al., 1991; Djordjevic et al., 1998; Djordjevic and Stefanovic, 1999; Cho, 2006; Hayami et al., 2008; Nowsheen et al., 2010). In particular, a number of articles and patents devoted to the analysis of Costas loops published by researchers and engineers from Finland (Vaelimaeki et al., 1996; Valimaki et al., 1998; Nissila et al., 2001; Kanwal et al., 2010).

Mathematical description and investigation of mathematical models of Costas loops is a very difficult task (Abramovitch, 2002). Direct description of these circuits leads to the analysis of nonlinear non-autonomous differential equations with high-frequency and low-frequency components in the right-hand sides of the equations (Leonov, 2006; Kudrewicz and Wasowicz, 2007; Leonov et al., 2009; Leonov, 2010; Kuznetsov, 2008). Because in the modern applications not only sinusoidal but many other classes of signal have been used (Henning, 1981; Wang and Emura, 1998; Sutterlin and Downey, 1999; Wang and Emura, 2001; Chang and Chen, 2008; Sarkar and Sengupta, 2010), it further complicates the study of

the corresponding differential equations.

Many methods of analysis of Costas loops are considered in various publications. However, the problems of development of adequate nonlinear models and rigorous analysis of such models are still far from being resolved. A simple linear analysis can lead to incorrect conclusions and, thereby, it requires rigorous justification. Numerical simulation is not a trivial task either due to the high-frequency properties of the signals involved. As mentioned in (Lai et al., 2005) **"in modern RF and mixed-signal designs (especially for SoCs) functional degradation of PLLs is a major cause of overall system malfunction, often resulting in many design and fabrication re-spins. Costs of such re-fabs can run into the millions of dollars and significantly delay product time-to-market"**. Therefore the development of nonlinear mathematical models of Costas loops is a must for the analysis of such systems.

A Costas loop is a PLL-based circuit and, thereby, methods similar to those used in the context of investigation of any PLL may be adapted here. The first mathematical description of physical models was proposed by Gardner (Gardner, 1966). These authors described a mathematical model of the BPSK Costas loop in the signal space and, without a rigorous mathematical justification, proposed a mathematical model in the phase space. Although PLL-based circuits are essentially nonlinear control systems, in the modern engineering literature devoted to the analysis of PLL-based circuits (Lindsey, 1972; Lindsey and Simon, 1973; Djordjevic et al., 1998; Djordjevic and Stefanovic, 1999; Fiocchi et al., 1992; Miyazaki et al., 1991; Cho, 2006; Wang and Leeb, 1987; Wang and Emura, 2001, 1998; Hayami et al., 2008; Young et al., 1992; Gardner et al., 1993; Gardner, 1993; Fines and Aghvami, 1991; Margaris, 2004; Kroupa, 2003; Razavi, 2003; Shu and Sanchez-Sinencio, 2005; Manassewitsch, 2005; Egan, 2000; Suarez and Quere, 2003; Tretter, 2007; Emura, 1982; Benarjee, 2006; Demir et al., 2000a; Stephens, 2001; Xanthopoulos et al., 2001; Demir et al., 2000b; Roberts et al., 2009; Kim et al., 2010; Tomkins et al., 2009; Proakis and Salehi, 2007), the main means of investigation include the use of simplified linear models, methods of linear analysis, empirical rules, and numerical simulation (see a plenary lecture of D. Abramovitch at the 2002 American Control Conference (Abramovitch, 2002)). While the analysis of linearized models of control systems may lead to incorrect conclusions[1] attempts to justify the reliability of conclusions, based on the application of such simplified approaches, are quite rare (see, e.g., (Suarez and Quere, 2003; Margaris, 2004; Banerjee and Sarkar, 2008a; Chicone and Heitzman, 2013; Best, 2007; Suarez

---

[1]   see, e.g. counterexamples to the filter hypothesis and to Aizerman's and Kalman's conjectures regarding absolute stability (Kuznetsov and Leonov, 2001, 2008; Kuznetsov et al., 2010; Leonov and Kuznetsov, 2010; Leonov et al., 2010,a,b; Bragin et al., 2010; Leonov and Kuznetsov, 2011a; Leonov et al., 2011a; Leonov and Kuznetsov, 2011b; Kuznetsov et al., 2011; Bragin et al., 2011; Leonov et al., 2011b; Kuznetsov et al., 2011; Leonov et al., 2011a; Kuznetsov et al., 2011; Leonov et al., 2011b, 2012, 2011b; Leonov and Kuznetsov, 2012; Kiseleva et al., 2012; Andrievsky et al., 2012; Kuznetsov et al., 2013; Leonov and Kuznetsov, 2013c,b,a, 2014, ISBN 978-1-908106-38-4; Kiseleva et al., 2014), Perron effects of sign inversions of Lyapunov exponents for time varying linearizations (Kuznetsov and Leonov, 2005; Leonov and Kuznetsov, 2007), etc.

et al., 2012; Feely, 2007; Feely et al., 2012; Kudrewicz and Wasowicz, 2007; Sarkar and Sengupta, 2010; Banerjee and Sarkar, 2008b)). A rigorous nonlinear analysis of a PLL-based circuit models is often a very difficult task (Leonov and Seledzhi, 2002; Kuznetsov, 2008; Kudrewicz and Wasowicz, 2007); therefore, for the analysis of nonlinear PLL models numerical simulations are widely used (Troedsson, 2009; Best, 2007; Bouaricha et al., 2012). However, for the high-frequency signals, complete numerical simulation of the physical model of a PLL-based circuit in signal/time space, described by nonlinear non-autonomous system of differential equations, is highly complicated since it is necessary to simultaneously observe "*very fast time scale of the input signals*" and "*slow time scale of signal's phases*" (Abramovitch, 2008b,a). Here, a relatively small discretization step in a numerical procedure does not allow one to consider transition processes for the high-frequency signals in a reasonable time period.

However, it is possible to overcome these difficulties through the development of the high-frequency asymptotic analysis methods (see (Leonov, 2008) and [PI–PVI,AXI]). These methods allow one to "split" high-frequency and low-frequency parts in the mathematical models of Costas loops in the space of signal phases. As noted in [PIV–PVI], this approach considers only a slow time scale of the signals phases. This requires the computation of the phase detector (PD) characteristic, which depends on waveforms of circuit signals (Leonov, 2008; Kuznetsov et al., 2009a,b, 2008; Leonov et al., 2006, 2009; Kuznetsov, 2008). In order to use the results of such analysis of a mathematical model describing the behaviour of the corresponding physical model, a rigorous justification is needed [PI–PVI]. To this end, it is essential, in turn, to apply also the averaging methods (Krylov and Bogolyubov, 1947; Mitropolsky and Bogolubov, 1961; Sanders et al., 2007; Artstein, 2007).

This work further contributes to the body of knowledge about Costas loops and it is devoted to the development and analysis of their mathematical models using the high-frequency asymptotic analysis approach. For the first time, a comprehensive rigorous mathematical method of constructing mathematical models of Costas loops for general signal waveforms is proposed. This method is based on the combination of engineering approaches to the investigation of PLL systems, the high-frequency analysis, and Fourier series application. The obtained results can be used for the analysis of the stability of Costas loops. The proposed numerical simulation method allows one to significantly reduce computation time spent on the numerical simulation of Costas loops (see patent application [AXII]). It has become possible to obtain important characteristics of Costas circuits such as pull-in time, pull-in range, etc. Also, the models developed facilitate further analysis and synthesis of Costas loops.

1.2 Structure of the work

In the next chapter operation principles of BPSK Costas loop with sinusoidal signals are considered. Then all necessary assumptions on every component of Costas circuit are made. These assumptions allow to derive a nonlinear model of BPSK Costas loop in phase space for general class of signal waveforms and to prove that this model is asymptotically equivalent to the physical model. Next another popular modification of Costas loop – QPSK Costas loop is considered. Similar results for QPSK Costas loop in phase space are obtained. Corresponding differential equations are derived in phase space and in signal space for both Costas loops. To prove that solutions of differential equations are similar averaging theory is applied to them in the next subsection.

Third chapter is devoted to the simulation of Costas loops in phase space and in signal space. First section describes software model of BPSK Costas loop. Then for different set of parameters and signal waveforms comparative simulation in both spaces is done. Next two sections describe simulation of QPSK Costas loop and establishe the dependency between the frequencies of signals and the accuracy of simulation in phase space.

1.3 Included articles and publications

The present work is based on publications [AI – AXVI] and included articles [PI – PVI].

At the first stage of the research, the BPSK Costas Loop with sinusoidal voltage-controlled oscillator was investigated for various input signal waveforms (sinusoidal, impulse, polyharmonic, piecewise-differentiable). These results were published in the included papers [PI–PII], where co-authors formulated the problems and the author formulated and proved theorems.

Then, to develop nonlinear mathematical models of the BPSK Costas loop for general class of input signal waveforms general theorems were developed based on [PV, PVI]. Theoretical results were extended and applied to QPSK Costas Loop. These results were published in the included papers [PIII–PIV]. The theoretical part of the justification of developed numerical simulation method for both modifications of Costas loops is due to the author.

Effective numerical procedure and software tool for the simulation and analysis of Costas loops have been proposed in Finnish patent application [AXII] and four Russian patents [AXIII–AXVI].

The main results of this work are also included in (Yuldashev, 2012, 2013a).

2 MATHEMATICAL MODELS OF COSTAS LOOPS

In this section following [PI–PIV,AVII,AXIII] and (Best, 2007; Lai et al., 2005; Yuldashev, 2012, 2013a) nonlinear mathematical models of BPSK Costas loop and QPSK Costas loop are considered.

2.1 Nonlinear models of BPSK Costas loop

Consider the BPSK Costas loop (Fig. 1) having sinusoidal Voltage-Controlled Oscillator (VCO) and sinusoidal carrier signals in lock state. The input signal is a
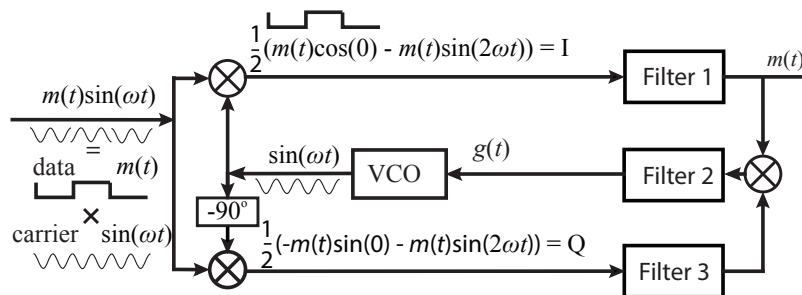
FIGURE 1   Costas loop after transient processes: $m(t)\sin(\omega t)$ is an input BPSK signal; $m(t) = (\pm 1)$ is the transmitted data; ω is the frequency of VCO output and input carrier signals

product of the transmitted data $m(t) = \pm 1$ and the sinusoidal carrier $\sin(\omega t)$ with the high frequency ω. After transient processes the carrier is synchronized with the VCO signal and there is no frequency difference between input carrier and VCO signal. On the lower branch (Q), the VCO signal is shifted by $-\frac{\pi}{2}$ and

then multiplied by the input signal

$$Q = m(t)\sin(\omega t)\sin(\omega t - \frac{\pi}{2}) =$$
$$= \frac{1}{2}\big(m(t)\sin(0) - m(t)\sin(2\omega t)\big) = \qquad (1)$$
$$= -\frac{1}{2}m(t)\sin(2\omega t).$$

The high-frequency part $\sin(2\omega t)$ in (1) is meant to be erased by a low-pass filter 3 on the Q branch. So, the signal on the lower branch after the filtration is equal to zero, which indicates that Costas loop is in-lock state.

On the upper branch (I), the input signal is multiplied by the output signal of VCO:

$$I = m(t)\sin(\omega t)\sin(\omega t) =$$
$$= \frac{1}{2}\big(m(t)\cos(0) - m(t)\cos(2\omega t)\big) =$$
$$= \frac{1}{2}\big(m(t) + m(t)\cos(2\omega t)\big).$$

Similarly to the Q branch, the term $\cos(2\omega t)$ is filtered by the Filter 1. Since $\cos(0) = 1$, on the upper branch, after filtration, one can obtain demodulated data $m(t)$. Then both branches are multiplied together and, after an additional low-pass filtration, one gets the signal $g(t)$ to adjust VCO frequency to the frequency of the input signal carrier. After the transient processes, the carrier and the VCO frequencies are equal to each other and the control input of VCO is equal to zero:

$$g(t) = 0.$$

Described principles, lacking rigorous mathematical justification, were well-known since Costas loop was invented (Costas, 1962) in the case of harmonic signals. One of the first effective mathematical models of high-frequency signals for PLL-based circuits was proposed in (Leonov, 2008) and [PV, PVI]. The included papers [PI–PIV] generalize this approach to the BPSK Costas loop with a harmonic VCO signal and various input carrier waveforms. Here, we will describe the general approach to the investigation of Costas loops.

Consider Costas loop before synchronization (see Fig. 2). i.e., the phases of the input carrier $\theta^1(t)$ and VCO $\theta^2(t)$ are different. Let us formulate the high-frequency property of signals $f^{1,2}(t) = f^{1,2}(\theta^{1,2}(t))$ (here $f^{1,2}(\theta)$ are waveforms) in the following way: suppose that there exist a large number ω_{min} such that for the frequencies[1]

$$\omega^{1,2}(t) = \dot{\theta}^{1,2}(t)$$

the following relation holds

$$\omega^{1,2}(t) \geq \omega_{min} > 0, \quad t \in [0, T], \qquad (2)$$

where T doesn't depend on ω_{min}.

---

[1] $\quad \dot{\theta}(t) = \frac{d\theta}{dt}$
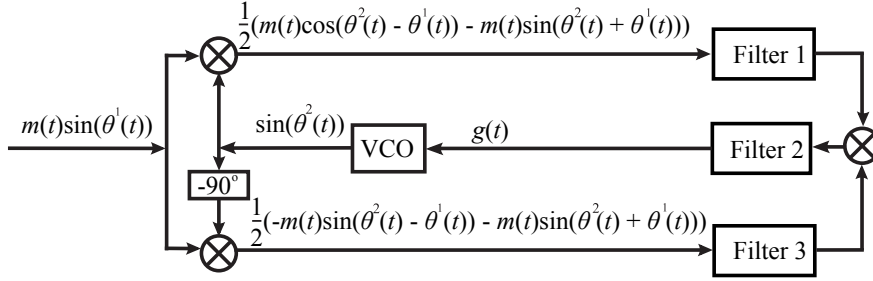
FIGURE 2   The BPSK Costas loop with the phase difference $\theta^2(t) - \theta^1(t)$

Suppose that for the frequencies

$$\left|\omega^1(t) - \omega^2(t)\right| \leq \Delta\omega, \ \forall t \in [0, T]. \tag{3}$$

Denote $\delta = \omega_{min}^{-\frac{1}{2}}$, then

$$
\begin{aligned}
&\left|\omega^p(t) - \omega^p(\tau)\right| \leq \Delta\Omega, \ p = 1, 2, \\
&|t - \tau| \leq \delta, \quad \forall t, \tau \in [0, T],
\end{aligned}
\tag{4}
$$

where $\Delta\Omega$ doesn't depend on δ.

In many applications (see, e.g. (Kaplan and Hegarty, 2006)) simplified Costas loop is used. Let us consider a circuit shown in Fig. 3, which is used in GPS. It is the same loop as in Fig. 2, yet without Filter 1 and Filter 3, $m(t) \equiv 1$.
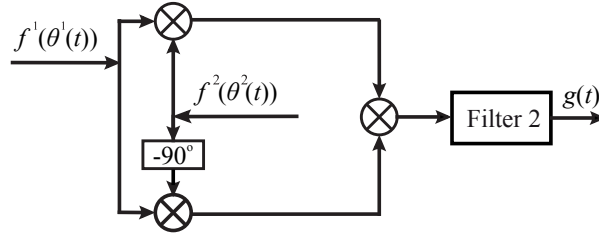
FIGURE 3   Simplified Costas loop circuit

For the piecewise differentiable signal waveforms $f^{1,2}(\theta)$, which can be presented in the form of Fourier series [2]

$$f^{1,2}(\theta) = \frac{a_0}{2} + \sum_{i=1}^{\infty} \left(a_i^{1,2} \cos(i\theta) + b_i^{1,2} \sin(i\theta) \right), \quad \theta \geq 0$$

where

$$a_0^p = \frac{1}{\pi} \int_{-\pi}^{\pi} f^p(\theta) d\theta, \ a_i^p = \frac{1}{\pi} \int_{-\pi}^{\pi} f^p(\theta) \cos(i\theta) d\theta,$$

$$b_i^p = \frac{1}{\pi} \int_{-\pi}^{\pi} f^p(\theta) \sin(i\theta) d\theta, \quad p = 1, 2,$$

---

[2]   full description of application of Fourier series to PLL-based systems can be found in (Yuldashev, 2013b)

it is possible to obtain a model of Costas loop in phase space. The linear filter can be described by the relation

$$\sigma(t) = \alpha_0(t) + \int_0^t \gamma(t-\tau)\xi(\tau)d\tau,$$

where $\xi(t)$ and $\sigma(t)$ are filter's input and output respectively. Most of the filters (Thede, 2005) satisfy the following condition

$$|\gamma(\tau) - \gamma(t)| = O(\delta), \quad |t - \tau| \le \delta, \quad \forall \tau, t \in [0, T], \tag{5}$$

where $\gamma(t)$ is the impulse transient function with bounded derivative. $\alpha_0(t)$ is exponentially damped function depending on the initial conditions of the filter.

By (5) we get

$$g(t) = \alpha_0(t) + \int_0^t \gamma(t-\tau)f^1(\theta^1(\tau))f^2(\theta^2(\tau))$$
$$f^1(\theta^1(\tau))f^2\left(\theta^2(\tau) - \frac{\pi}{2}\right)d\tau.$$

Consider the block-diagram shown in Fig. 4.
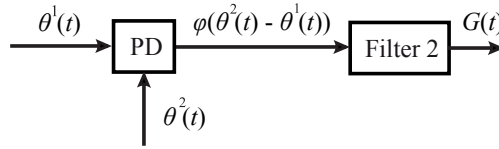
FIGURE 4   Phase detector and filter

Here, the phase detector (PD) is a nonlinear element with the output $\varphi(\theta^1(t) - \theta^2(t))$ and Filter 2 is the same as in Fig. 3. Let their initial conditions also be the same, then

$$G(t) = \alpha_0(t) + \int_0^t \gamma(t-\tau)\varphi(\theta^1(\tau) - \theta^2(\tau))d\tau. \tag{6}$$

Consider a 2π-periodic function

$$\varphi(\theta) = \frac{A_0^1 A_0^2}{4} + \frac{1}{2}\sum_{l=1}^{\infty}\Big((A_l^1 A_l^2 + B_l^1 B_l^2)\cos(l\theta) +$$
$$+ (A_l^1 B_l^2 - B_l^1 A_l^2)\sin(l\theta)\Big), \tag{7}$$

where A_l^p, B_l^p can be calculated from the Fourier series coefficients of $f^{1,2}(\theta)$ as follows

$$A_l^1 = \frac{a_0^1 a_l^1}{2} + \frac{1}{2}\sum_{m=1}^{\infty}[a_m^1(a_{m+l}^1 + a_{m-l}^1) + b_m^1(b_{m+l}^1 + b_{m-l}^1)],$$

$$B_l^1 = \frac{a_0^1 b_l^1}{2} + \frac{1}{2}\sum_{m=1}^{\infty}[a_m^1(b_{m+l}^1 - b_{m-l}^1) - b_m^1(a_{m+l}^1 - a_{m-l}^1)],$$

$$A_l^2 = \frac{a_0^2 \alpha_l^2}{2} + \frac{1}{2}\sum_{m=1}^{\infty}[\alpha_m^2(\alpha_{m+l}^2 + \alpha_{m-l}^2) + \beta_m^2(\beta_{m+l}^2 + \beta_{m-l}^2)],$$ (8)

$$B_l^2 = \frac{a_0^2 \beta_l^2}{2} + \frac{1}{2}\sum_{m=1}^{\infty}[\alpha_m^2(\beta_{m+l}^2 - \beta_{m-l}^2) - \beta_m^2(\alpha_{m+l}^2 - \alpha_{m-l}^2)],$$

where

$$\alpha_k^2 = \begin{cases} a_k^2, & k = 4p, \\ b_k^2, & k = 4p+1, \\ -a_k^2, & k = 4p+2, \\ -b_k^2, & k = 4p+3, \end{cases} \quad \beta_k^2 = \begin{cases} b_k^2, & k = 4p, \\ -a_k^2, & k = 4p+1, \\ -b_k^2, & k = 4p+2, \\ a_k^2, & k = 4p+3, \end{cases}$$ (9)

$$a_{-h} = a_h, \quad b_{-h} = b_h, \quad h < 0.$$

The following theorem proves the asymptotic equivalence of the models shown in Fig. 3 and Fig. 4.

Theorem 1. *If (2)–(5), are satisfied then*

$$|g(t) - G(t)| = O(\delta), \quad \forall t \in [0, T].$$ (10)

The proof of this theorem based on analysis of Fourier series can be found in the included articles [PI–PIV].

To illustrate how to use this theorem the following table (TABLE 1) provides phase-detector characteristics for the most common signal waveforms.

Remark

Since waveforms $f^{1,2}(\theta)$ are piecewise-differentiable their Fourier coefficients $a_n^{1,2}$ and $b_n^{1,2}$ tends to zero

$$a_n^{1,2} = O(\frac{1}{n}), \quad b_n^{1,2} = O(\frac{1}{n}).$$

By (8) Fourier coefficients of function $\varphi(\theta)$ satisfy relation
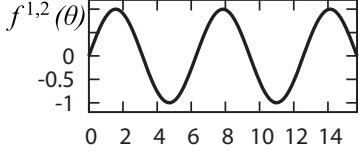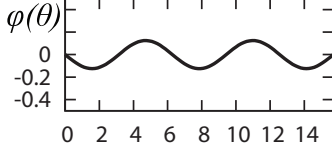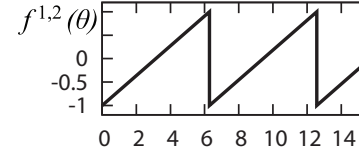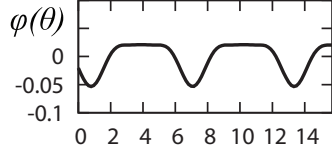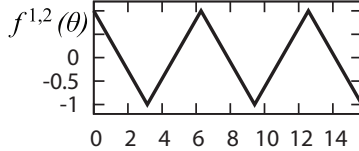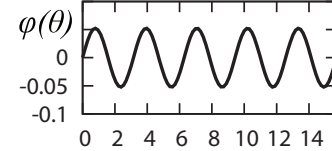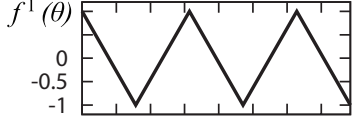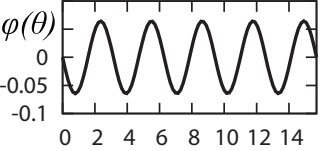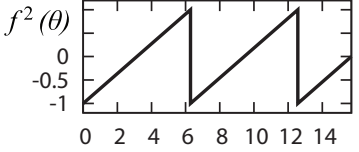
$$A_n^{1,2} = O(\frac{1}{n^2}), \quad B_n^{1,2} = O(\frac{1}{n^2}).$$ (11)

Condition (11) guaranties that $\varphi(\theta)$ is continuous.

2.2 QPSK Costas loop

One of the most popular Costas loop based circuit is QPSK Costas loop (Waters, 1982; Ryan and Stilwell, 1978). It is used in biomedical applications (Iniewski,

TABLE 1   Phase detector characteristics examples

$f^{1,2}(\theta) = \sin(\theta),\ \varphi(\theta) = -\frac{1}{8}\sin(2\theta)$
$f^{1,2}(\theta) = -\frac{2}{\pi}\sum\limits_{n=1}^{\infty}\frac{1}{n}\sin\left(n\theta\right),$ $\varphi(\theta) = \frac{-1}{72} + \frac{1}{2}\sum\limits_{l=1}^{\infty}\begin{cases}\frac{16}{\pi^4 l^4}\cos(l\theta), & l = 4p,\ p \in \mathbb{N} \\ \frac{-4(\pi l-2)}{\pi^4 l^4}\cos(l\theta)\frac{-4(\pi l-2)}{\pi^4 l^4}\sin(l\theta), & l = 4p+1,\ p \in \mathbb{N}_0 \\ \frac{-8}{\pi^3 l^3}\sin(l\theta), & l = 4p+2,\ p \in \mathbb{N}_0 \\ \frac{4(\pi l+2)}{\pi^4 l^4}\cos(l\theta)\frac{-4(\pi l+2)}{\pi^4 l^4}\sin(l\theta), & l = 4p+3,\ p \in \mathbb{N}_0\end{cases}$
$f^{1,2}(\theta) = \frac{8}{\pi^2}\sum\limits_{n=1}^{\infty}\frac{1}{(2n-1)^2}\cos\left((2n-1)\theta\right)$ $\varphi(\theta) = \frac{512}{\pi^5}\sum\limits_{l=1}^{\infty}\frac{1}{(4l+2)^5}\sin((4l+2)\theta)$
$f^{1}(\theta) = \frac{8}{\pi^2}\sum\limits_{n=1}^{\infty}\frac{1}{(2n-1)^2}\cos\left((2n-1)\theta\right)$ $f^{2}(\theta) = -\frac{2}{\pi}\sum\limits_{n=1}^{\infty}\frac{1}{n}\sin\left(n\theta\right)$ $\varphi(\theta) = \frac{-1}{72} + \frac{8}{\pi^2}\sum\limits_{l=1}^{\infty}\begin{cases}\frac{4}{\pi^2(l+4)^4}\cos((l+4)\theta), & l = 4p, \\ -\frac{2}{\pi l^3}\sin(l\theta), & l = 4p+2, \\ 0, & l = 2p+1,\ p \in \mathbb{N}_0\end{cases}$

2008), wireless communication (Tranter, 2001), Internet of Things (Agbinya, 2011), e.t.c. Below, we provide a rigorous mathematical description of the QPSK Costas loop and formulate the corresponding theorem. The following description of the QPSK Costas loop follows article [PIV].

Consider the QPSK Costas loop shown in Fig. 5.
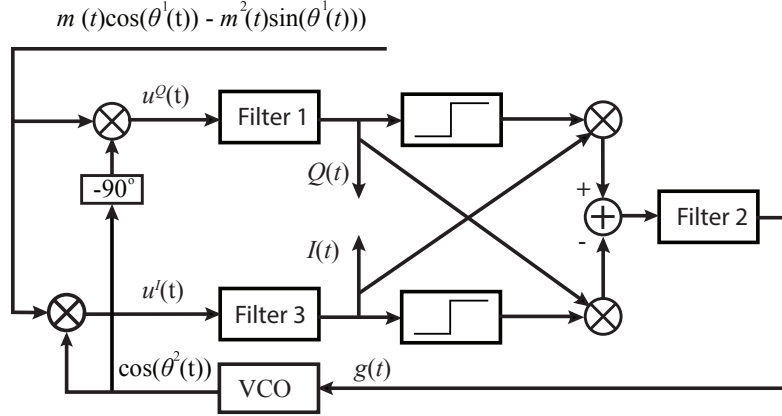
FIGURE 5   The QPSK Costas loop

The input signal has the form

$$m^1(t)\cos(\theta^1(t)) - m^2(\sin(\theta^1(t))),$$

where $m^{1,2}(t) = \pm 1$ is the transmitted data, $\sin(\theta^1(t))$ and $\cos(\theta^1(t))$ are carriers. The output of the VCO is supposed to be sinusoidal $\cos(\theta^2(t))$. Both input signal and output signal of VCO are high-frequency signals, i.e., requirements (2)–(4) are met.

On the lower branch (I), after the multiplying input signal by the VCO signal, we get

$$u^I(t) = \left(m^1(t)\cos(\theta^1(t)) - m^2(\sin(\theta^1(t)))\right)\cos(\theta^2(t)),$$

After filtering by a low-pass filter (Filter 3) we get

$$I(t) = \int_0^t h(t-\tau)u^I(\tau)d\tau,$$

where $h(t-\tau)$ is an impulse transient function of the Filter. This signal is used to obtain one of the carriers of the input signal. On the Q branch the product of the input signal and the VCO signal, shifted by -90°, forms the signal

$$u^Q(t) = \left(m^1(t)\cos(\theta^1(t)) - m^2(\sin(\theta^1(t)))\right)\sin(\theta^2(t)).$$

Then the output of Filter 1 is

$$Q(t) = \int_0^t h(t-\tau)u^Q(\tau)d\tau.$$

This signal allows to get the second carrier. After the filtration, both signals, $I(t)$ and $Q(t)$, pass through the limiters. Then the outputs of the limiters $\text{sign}(I(t))$ and $\text{sign}(Q(t))$ are multiplied as shown in Fig. 5. The resulting signal, after the filtration by Filter 2, forms the control signal $g(t)$ for the VCO. Similarly to the BPSK Costas loop, Filter 2 satisfies conditions (5).

According to (Kaplan and Hegarty, 2006) described circuit is usually simplified and we may consider a modified loop (see Fig. 6). Here $m^{1,2}(t) \equiv 1$.
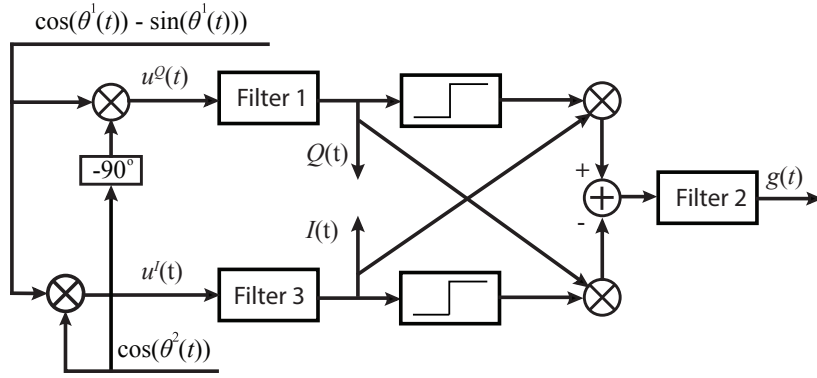
FIGURE 6   A simplified QPSK Costas loop

Suppose that Filter 1 and Filter 3 satisfy the conditions[3] (Leonov and Kuznetsov, 2014, ISBN 978-1-908106-38-4)

$$
\begin{aligned}
\int_0^t h(t-\tau)\sin(\omega\tau+\theta_0)d\tau &= O(\frac{1}{\omega}), \ \forall \omega > \omega_{min}, \\
\int_0^t h(t-\tau)\sin(\omega\tau+\theta_0)d\tau &= \sin(\omega\tau+\theta_0) + O(\frac{1}{\omega}), \ \forall \omega < \Delta\omega.
\end{aligned}
\tag{12}
$$

Consider the block-scheme shown in Fig. 4, where Filter 2 is the same filter as the one in Fig. 6

Consider a 2π-periodic function $\varphi(\theta)$

$$
\begin{aligned}
\varphi(\theta) = \frac{\sqrt{2}}{2}\Big(&\sin(\theta(t)+\frac{\pi}{4})\,\text{sign}(\sin(\theta(t)-\frac{\pi}{4})) - \\
& - \sin(\theta(t)-\frac{\pi}{4})\,\text{sign}(\sin(\theta(t)+\frac{\pi}{4}))\Big)
\end{aligned}
\tag{13}
$$

The following theorem allows one to justify the transition from the block-scheme shown in Fig. 6 to that of Fig. 4.

Theorem 2. *If conditions (2)–(5) and (12) are satisfied, then*

$$
|g(t) - G(t)| = O(\delta), \quad \forall t \in [0, T].
\tag{14}
$$

---

[3]   relation between δ and ω_{min} is the same as before: $\delta = \omega_{min}^{-\frac{1}{2}}$

This theorem can be proved similarly to the previews theorem by dividing time interval $[0, T]$ on sufficiently small subintervals and estimating corresponding integrals.

2.3 Differential equations of Costas loops

From a mathematical point of view, linear filter can also be described by a system of linear differential equations

$$\frac{dx}{dt} = Ax + b\xi(t),$$
$$\sigma(t) = c^* x, \tag{15}$$

a solution of which takes the form (5). Here A is the constant $n \times n$ matrix of the filter, $x(t)$ represents the state of the filter, b and c are constant $\mathbb{R}^n$ vectors — parameters of the filter, $\xi(t)$ — input of the filter, $\sigma(t)$ — output of the filter, * is the transpose operator. The model of tunable generator is usually assumed to be linear (Kroupa, 2003; Best, 2007; Chen et al., 2012):

$$\frac{d\theta^2}{dt} = \omega_{free}^2 + LG(t),$$
$$t \in [0, T], \tag{16}$$

where is a free-running frequency of the tunable generator and L is an oscillator gain. Similarly, one can consider various nonlinear models of VCO (see, e.g., [Lai et al., 2005]). Suppose that the frequency of input signal carrier is constant. By equations of filter (15) and VCO (16) one has

$$\frac{dx}{dt} = Ax + bf^1(\theta^1(t))f^2(\theta^2(t))f^1(\theta^1(t))f^2(\theta^2(t) - \frac{\pi}{2}),$$
$$\frac{d\theta^2}{dt} = \omega_{free}^2 + Lc^* x, \tag{17}$$
$$\frac{d\theta^1}{dt} \equiv \omega^1.$$

Similarly the QPSK Costas loop can be described by the following differential equations:

$$\frac{dx_1}{dt} = A_1 x_1 + b_1(\cos(\theta^2(t))(\cos(\theta^1(t)) - \sin(\theta^1(t)))),$$
$$\frac{dx_2}{dt} = A_2 x_2 + b_2(\text{sign}(c_1^* x_1)(c_3^* x_3) - \text{sign}(c_3^* x_3)(c_1^* x_1)),$$
$$\frac{dx_3}{dt} = A_3 x_3 + b_3(\sin(\theta^2(t))(\cos(\theta^1(t)) - \sin(\theta^1(t)))), \tag{18}$$
$$\frac{d\theta^1}{dt} \equiv \omega^1,$$
$$\frac{d\theta^2}{dt} = \omega_{free}^2 + Lc_2^* x_2,$$

where $A_{1,2,3}$, $b_{1,2,3}$, $c_{1,2,3}$ are parameters of the filter and $x_{1,2,3}(t)$ is the state of the filter.

Using the phase-detector characteristics, it is possible to derive differential equations of Costas loops in the phase space as follows

$$
\begin{aligned}
\frac{dx}{dt} &= Ax + b\varphi(\theta_\Delta(t)), \\
\frac{d\theta_\Delta}{dt} &= \omega_{free}^2 - \omega^1 + Lc^*x, \\
\theta_\Delta(t) &= \theta^2(t) - \theta^1(t).
\end{aligned}
\tag{19}
$$

Here $\varphi(\theta)$ is the phase detector characteristics, which depends on the signal wave-forms.

The averaging methods allow one to justify that the solutions of differential equations in the phase space are close to the solutions in the signal/time space. These methods are described in the next section.

2.4 Averaging method for investigation of Costas loops

The averaging method was invented to solve problems of celestial mechanics. History and development of this method up to 1960s is described in (Mitropolsky, 1967). Main theoretical results from this book were obtained by Krylov, Bogoliubov, and Mitropolsky became classical in averaging theory. Contemporary results can be found in (Sanders et al., 2007).

Lets apply the averaging method to the Costas loop equations. Original system (17) is equivalent to the system

$$
\begin{aligned}
\frac{dx}{dt} &= Ax + bf^1(\omega^1 t)f^2(\omega^1 t + \theta_\Delta(t))f^1(\omega^1 t)f^2(\omega^1 t + \theta_\Delta(t) - \frac{\pi}{2}), \\
\frac{d\theta_\Delta}{dt} &= \omega_\Delta + Lc^*x,
\end{aligned}
\tag{20}
$$

where $\theta_\Delta = \theta^2 - \theta^1$ is the phase difference of VCO and input carrier and ω_Δ is initial frequency difference. To apply the averaging theory to this system we have to convert it to the standard form

$$
\frac{dy}{dt} = \varepsilon F(y, t), \quad y(0) = y_0,
\tag{21}
$$

where ε is a small parameter. Since frequencies $\omega^{1,2}$ are assumed to be large, it is reasonable to put $\varepsilon = \frac{1}{\omega^1}$. Denote

$$
\begin{aligned}
\tau &= \omega^1 t, \\
z(\tau) &= x(\frac{\tau}{\omega^1}) = x(t),
\end{aligned}
\tag{22}
$$

then system (20) transforms to

$$\frac{dz}{d\tau} = \frac{1}{\omega^1}\left(Az + bf^1(\tau)f^2(\theta_\Delta + \tau)f^1(\tau)f^2(\theta_\Delta + \tau - \frac{\pi}{2})\right),$$
$$\frac{d\theta_\Delta}{d\tau} = \frac{1}{\omega^1}\left(\omega_\Delta + Lc^*z\right).$$
(23)

2.4.1 First order periodic averaging

The following theorem allows to obtain easily the phase-detector characteristics for sinusoidal signals without asymptotic analysis given in the previous sections. General averaging theorems described in the next subsections can not be applied to Costas loop equations directly because they require theorem 1 and theorem 2 to be proved.

Consider an equation (21) where F is T-periodic on t and Lipschitz continuous[4]. Let D be an bounded open set, containing x_0, choose ε_0 such that $0 < \varepsilon \leq \varepsilon_0$. Let us introduce the averaged equation

$$\frac{dz}{dt} = \varepsilon\bar{F}(z), \quad z(0) = x_0,$$
(24)

where

$$\bar{F}(z) = \frac{1}{T}\int_0^T F(z,t)dt.$$
(25)

There is a constant L such that solutions $z(t,\varepsilon)$ and $x(t,\varepsilon)$ remain in D if $0 \leq t \leq \frac{L}{\varepsilon}$.

Theorem 3. *Suppose that ε_0, D, and L are as above. Then there exists a constant $c > 0$ such that*

$$||y(t,\varepsilon) - z(t,\varepsilon)|| < c\varepsilon$$

for $0 \leq \varepsilon \leq \varepsilon_0$ and $0 \leq t \leq \frac{L}{\varepsilon}$.

Proof of this theorem can be found in (Sanders et al., 2007) (p. 31). This theorem allows one to obtain phase-detector characteristics for Costas loop with sinusoidal signal waveforms

$$f^{1,2}(\theta) = \sin(\theta).$$

System (23) for these waveforms equals to

$$\frac{dz}{d\tau} = \frac{1}{\omega^1}\left(Az + b\sin(\tau)\sin(\theta_\Delta(\tau) + \tau)\sin(\tau)\sin(\theta_\Delta(\tau) + \tau - \frac{\pi}{2})\right),$$
$$\frac{d\theta_\Delta}{d\tau} = \frac{1}{\omega^1}\left(\omega_\Delta + Lc^*z\right).$$
(26)

Obviously the right-hand side of system (26) is Lipschitz continuous and 2π periodic. As before

$$\varepsilon = \frac{1}{\omega^1}.$$

---

[4] $|F(y_1, t) - F(y_2, t)| \leq K|y_1 - y_2|$, where k is a certain constant

The choice of the time interval obviously defines the constant L and the domain D ((Sanders et al., 2007). To obtain the averaged equation (24) we need to integrate the right-hand side

$$\frac{1}{2\pi}\int_0^{2\pi} Az + b\sin(\tau)\sin(\theta_\Delta + \tau)\sin(\tau)\sin(\theta_\Delta + \tau - \frac{\pi}{2})d\tau =$$

$$= Az + \frac{b}{2\pi}\int_0^{2\pi}\left(\frac{1}{2}(1+\cos(2\tau))\sin(\theta_\Delta + \tau)\cos(\theta_\Delta + \tau)\right)d\tau =$$

$$= Az + \frac{b}{8\pi}\int_0^{2\pi}((1+\cos(2\tau))(\sin(2\theta_\Delta + 2\tau)))d\tau = \tag{27}$$

$$= Az + \frac{b}{8}\sin(2\theta_\Delta),$$

$$\frac{1}{2\pi}\int_0^{2\pi}(\omega_\Delta + Lc^*z)d\tau = \omega_\Delta + Lc^*z.$$

So, by (22) we get the averaged equation of Costas loop for sinusoidal signals

$$\frac{dx}{dt} = Ax + \frac{b}{8}\sin(\theta_\Delta(\tau)),$$
$$\dot{\theta}_\Delta = \omega_\Delta + Lc^*x,$$

which is equals to the equation of Costas Loop in phase space with phase-detector characteristics $\varphi(\theta) = \frac{1}{8}\sin(2\theta)$.

However, it is not obvious how to apply this theorem to obtain PD characteristics for other signal waveforms. In the following subsection we will consider general averaging theory and apply it to the Costas loops with non-sinusoidal waveforms.

2.4.2 General averaging

Here we will follow a recent approach presented in (Artstein, 2007).

Definition 1. *Let M be a complete metric space with its metric $d(\cdot,\cdot)$. Mapping $S : M \to M$ is called a contraction, with contraction factor ρ, if $\rho < 1$ and $d(S(v), S(w)) < \rho d(v, w)$ for all v and w in M.*

Lemma 1. *Let $S^1 : M \to M$ be a contraction, with a contraction factor $\rho < 1$. Let $S^2 : M \to M$ be another mapping such that*

$$d(S^1(v), S^2(v)) \le \delta \tag{28}$$

for every $v \in M$. Then the distance between the unique fixed point v^1 of S^1 and every fixed point v^2 of S^2 is less than or equal to $\delta(1-\rho)^{-1}$.

Proof. By the contraction property of S^1

$$d(v^1, S^1(v^2)) = d(S^1(v^1), S^1(v^2)) \leq \rho d(v^1, v^2) \tag{29}$$

From condition (28) we get

$$d(S^2(v^1), v^2) = d(S^2(v^1), S^2(v^2)) \leq \delta \tag{30}$$

Inequalities (29) and (30) combined with triangular inequality applied to points v^1, v^2, and $S^1(v^2)$ finalize the proof. $\qquad\square$

Consider mapping $S(y(\cdot)) : C([0,T], \mathbb{R}^n) \to C([0,T], \mathbb{R}^n)$ given by

$$S(y(\cdot))(t) = y_0 + \varepsilon \int\limits_0^t F(y(\tau), \tau) d\tau. \tag{31}$$

Function $y(\cdot)$ is a solution of (21) if and only if it is a fixed point of the mapping $S(y(\cdot))$. Furthermore, in case of Costas loop the function $F(y,t)$ is bounded, say by r, then solutions of (21) are Lipschitz with respect to the time variable with Lipschitz constant εr. Let's introduce a new norm to make mapping (31) a contraction.

Lemma 2. *Consider equation* (21) *and assume that the right-hand side is K-Lipschitz in y, i.e.*

$$|F(y_1, t) - F(y_2, t)| \leq K|y_1 - y_2|.$$

Then the mapping $S(y(\cdot))$ given by (31) is a contraction with respect to the norm

$$||y(\cdot)||_l = \max_{t \in [0,T]} |y(t)| e^{-Kt}.$$

This norm is equivalent to the sup *norm. The contraction factor is estimated by*

$$\rho = \varepsilon(1 - e^{-KT}).$$

Proof. Let t_m be a point where $||S(y_1(\cdot)) - S(y_2(\cdot))||_l$ reaches its maximum on the interval $[0, T]$. Then using Lipschitz condition we get

$$||S(y_1(\cdot)) - S(y_2(\cdot))||_l = e^{-Kt_m} \left| \int\limits_0^{t_m} (F(y_1(\tau), \tau) - F(y_2(\tau), \tau) d\tau \right| \leq$$

$$\leq e^{-Kt_m} \int\limits_0^{t_m} K\varepsilon |y_1(\tau) - y_2(\tau)| d\tau \leq$$

$$\leq e^{-Kt_m} ||y_1(\cdot) - y_2(\cdot)||_l \int\limits_0^{t_m} K\varepsilon e^{K\tau} d\tau =$$

$$= e^{-Kt_m} ||y_1(\cdot) - y_2(\cdot)||_l \varepsilon (e^{Kt_m} - 1) =$$

$$= \varepsilon ||y_1(\cdot) - y_2(\cdot)||_l (1 - e^{-Kt_m}) \leq$$

$$\leq \varepsilon ||y_1(\cdot) - y_2(\cdot)||_l (1 - e^{-KT})$$

Since

$$||y(\cdot)||_l = \max_{t \in [0,T]} |y(t)|e^{-Kt} \leq \max_{t \in [0,T]} |y(t)| \leq \max_{t \in [0,T]} |y(t)|e^{-Kt+KT} = e^{KT}||y(\cdot)||_l$$

holds then $|| \cdot ||_l$ norm is equivalent to the sup norm. □

Corollary 1. *Consider two differential equations of the form* (21) *with right-hand sides* $F^1(y,t)$ *and* $F^2(y,t)$ *on the interval* $[0,T]$. *Let* $S^{1,2}(y(\cdot))$ *be the corresponding mappings*

$$S^{1,2}(y(\cdot))(t) = y_0 + \varepsilon \int_0^t F^{1,2}(y(\tau),\tau)d\tau.$$

Suppose that $F^1(y,t)$ *is K-Lipschitz in the state* y, $F^{1,2}(y,t)$ *are bounded by* r, *and*

$$|S^1(y(\cdot))(t) - S^2(y(\cdot))(t)| \leq \delta$$

holds for every r-Lipschitz function $y(\cdot)$ *with initial condition* $y(0) = y_0$. *Then*

$$\max_{t \in [0,T]} |y^1(t) - y^2(t)| \leq e^{2KT}\delta,$$

where $x^1(t)$ *is the unique solution of* $\frac{dy}{dt} = \varepsilon F^1(y,t)$ *and* $x^2(t)$ *is a solution of* $\frac{dy}{dt} = \varepsilon F^2(y,t)$.

Proof. Both of the right-hand sides $F^{1,2}(y,t)$ are bounded by r, so corresponding solutions are r-Lipschitz. Since $F^1(y,t)$ is K-Lipschitz then by Lemma 2 corresponding mapping $S^1(y(\cdot))$ of r-Lipschitz functions from $[0,T]$ to $\mathbb{R}^n$ is a contraction with respect to its $|| \cdot ||_l$ norm with a contraction factor

$$\varepsilon(1 - e^{-KT}) \leq (1 - e^{-KT}).$$

By Lemma 1 we have

$$||y^1(t) - y^2(t)||_l \leq \delta(1-\rho)^{-1} \leq \delta e^{KT}.$$

Lets multiply both sides of this inequality by e^{KT}

$$e^{KT}||y^1(t) - y^2(t)||_l \leq \delta e^{2KT}.$$

Inequality $\max_{t \in [0,T]} |y(t)| \leq e^{KT}||y(\cdot)||_l$ finalizes the proof. □

Consider equation (21) where $y \in \mathbb{R}^n$, $t \in [0.\infty)$, and $F(y,t)$ is continuous. For the averaged system (24) function $\bar{F}(z)$ is defined by the following equation

$$\bar{F}(z) = \lim_{T \to \infty} \frac{1}{T} \int_{t_0}^{t_0+T} F(z,\tau)d\tau, \tag{32}$$

where the limit in (32) is assumed uniform in $t_0 \geq 0$. Notice that this average may not exist. When an equation has this average we look for non-negative numbers $\Delta(\varepsilon)$ and $\eta(\varepsilon)$ with the property

$$\frac{\varepsilon}{\Delta(\varepsilon)} \left| \int_{t_0}^{t_0 + \frac{\Delta(\varepsilon)}{\varepsilon}} (F(y, \tau) - \bar{F}(y)) \, d\tau \right| \leq \eta(\varepsilon), \quad \forall y, \quad 0 \leq t_0 \leq \varepsilon^{-1}(1 - \Delta(\varepsilon)).$$

Denote $s = \varepsilon t$ then

$$\frac{1}{\Delta(\varepsilon)} \left| \int_{s_0}^{s_0 + \Delta(\varepsilon)} \left(F(y, \frac{s}{\varepsilon}) - \bar{F}(y) \right) ds \right| \leq \eta(\varepsilon), \quad \forall y, \quad 0 \leq s_0 \leq 1 - \Delta(\varepsilon). \tag{33}$$

Pair $(\Delta(\varepsilon), \eta(\varepsilon))$ is called the rate of averaging.

Theorem 4. *Assume that the function $F(y, t)$ is K-Lipschitz in y and bounded by r. Suppose that the equation has a time-independent average $\bar{F}(z)$ and let $(\Delta(\varepsilon), \eta(\varepsilon))$ be a rate of averaging. Then*

$$|y(t) - z(t)| \leq T e^{2KT} ((K+2) r \Delta(\varepsilon) + \eta(\varepsilon))$$

namely, it is of order $\max(\Delta(\varepsilon), \eta(\varepsilon))$, this uniformly for t in the interval $[0, \varepsilon^{-1}]$.

Proof. Lets apply the change of variable $s = \varepsilon t$. Then equations (21) and (24) transforms to

$$\frac{dy}{ds} = F(y, \frac{s}{\varepsilon}), \quad y(0) = y_0,$$

and

$$\frac{dz}{ds} = \bar{F}(z), \quad z(0) = y_0.$$

Lets estimate the following integral

$$\left| \int_0^s (F(y(\sigma), \frac{\sigma}{\varepsilon})) - \bar{F}(y(\sigma))) d\sigma \right|$$

using K-Lipschitz properties of $F(y,t)$ and $\bar{F}(z)$:

$$\left| \int_0^s (F(y(\sigma), \frac{\sigma}{\varepsilon})) - \bar{F}(y(\sigma))) d\sigma \right| \leq$$

$$\leq \sum_{k=0}^{\lfloor \frac{s}{\Delta(\varepsilon)} \rfloor} \int_{k\Delta(\varepsilon)}^{(k+1)\Delta(\varepsilon)} \left| F(y(\sigma), \frac{\sigma}{\varepsilon})) - \bar{F}(y(\sigma)) \right| d\sigma + 2rT\Delta(\varepsilon) \leq$$

$$\leq \sum_{k=0}^{\lfloor \frac{s}{\Delta(\varepsilon)} \rfloor} \Big(\int_{k\Delta(\varepsilon)}^{(k+1)\Delta(\varepsilon)} \left| F(y(\sigma), \frac{\sigma}{\varepsilon})) - F(y(\frac{2k+1}{2}\Delta(\varepsilon)), \frac{\sigma}{\varepsilon})) \right| d\sigma +$$

$$+ \int_{k\Delta(\varepsilon)}^{(k+1)\Delta(\varepsilon)} \left| F(y(\frac{2k+1}{2}\Delta(\varepsilon)), \frac{\sigma}{\varepsilon})) - \bar{F}(y(\frac{2k+1}{2}\Delta(\varepsilon))) \right| d\sigma +$$

$$+ \int_{k\Delta(\varepsilon)}^{(k+1)\Delta(\varepsilon)} \left| \bar{F}(y(\frac{2k+1}{2}\Delta(\varepsilon))) - \bar{F}(y(\sigma)) \right| d\sigma \Big) + 2rT\Delta(\varepsilon) \leq$$

$$\leq \sum_{k=0}^{\lfloor \frac{s}{\Delta(\varepsilon)} \rfloor} \Big(K\frac{r\Delta(\varepsilon)}{2} +$$

$$+ \int_{k\Delta(\varepsilon)}^{(k+1)\Delta(\varepsilon)} \left| F(y(\frac{2k+1}{2}\Delta(\varepsilon)), \frac{\sigma}{\varepsilon})) - \bar{F}(y(\frac{2k+1}{2}\Delta(\varepsilon))) \right| d\sigma +$$

$$+ K\frac{r\Delta(\varepsilon)}{2} \Big) + 2rT\Delta(\varepsilon) \leq$$

$$\leq TKr\Delta(\varepsilon) + 2rT\Delta(\varepsilon) +$$

$$+ \sum_{k=0}^{\lfloor \frac{s}{\Delta(\varepsilon)} \rfloor} \int_{k\Delta(\varepsilon)}^{(k+1)\Delta(\varepsilon)} \left| F(y(\frac{2k+1}{2}\Delta(\varepsilon)), \frac{\sigma}{\varepsilon})) - \bar{F}(y(\frac{2k+1}{2}\Delta(\varepsilon))) \right| d\sigma$$

By (33) it is possible to estimate last sum of integrals

$$\sum_{k=0}^{\lfloor \frac{s}{\Delta(\varepsilon)} \rfloor} \int_{k\Delta(\varepsilon)}^{(k+1)\Delta(\varepsilon)} \left| F(y(\frac{2k+1}{2}\Delta(\varepsilon)), \frac{\sigma}{\varepsilon})) - \bar{F}(y(\frac{2k+1}{2}\Delta(\varepsilon))) \right| d\sigma \leq$$

$$\leq \sum_{k=0}^{\lfloor \frac{s}{\Delta(\varepsilon)} \rfloor} \eta(\varepsilon)\Delta(\varepsilon) \leq T\eta(\varepsilon)$$

Last two equations give the following estimate

$$\left| \int_0^s (F(y(\sigma), \frac{\sigma}{\varepsilon})) - \bar{F}(y(\sigma))) d\sigma \right| \leq T((2+K)r\Delta(\varepsilon) + \eta(\varepsilon)). \tag{34}$$

Combination of the (34) and corollary 1 completes the proof. $\qquad \square$

Now we can apply this theorem to the Costas loops with K-Lipschitz signal waveforms on time interval $[0, T]$. Consider an original system (20) of Costas Loop. Time independent average is equal to

$$
\frac{dx}{dt} = Ax + b\varphi(\theta_\Delta(t)),
$$
$$
\frac{\theta_\Delta}{dt} = \omega_\Delta + Lc^*x.
$$

(35)

Theorem 1 provides the function φ and the averaging rate $(O(\varepsilon^{\frac{1}{4}}), O(\varepsilon^{\frac{1}{4}}))$, i.e.

$$
\left| \int_{s_0}^{s_0+\varepsilon^{\frac{1}{4}}} \left(f^1(\omega^1 t) f^2(\omega^1 t + \theta_\Delta) f^1(\omega^1 t) f^2(\omega^1 t + \theta_\Delta - \frac{\pi}{2}) - \varphi(\theta_\Delta) \right) dt \right| \le O\left(\sqrt{\varepsilon}\right),
$$

$\forall s_0, \quad 1 \le s_0 + 1 \le T.$

By theorem 4 solutions of the equation of Costas loop in signal space (20) and in phase space (35) are close in the following sense

$$
|x(t) - z(t)| = O(\varepsilon^{\frac{1}{4}}), \quad t \in [0, T].
$$

Recall equations of QPSK Costas loop in signal space (18)

$$
\frac{dx_1}{dt} = A_1 x_1 + b_1(\cos(\theta^2(t))(\cos(\theta^1(t)) - \sin(\theta^1(t)))),
$$
$$
\frac{dx_2}{dt} = A_2 x_2 + b_2(\text{sign}(c_1^* x_1)(c_3^* x_3) - \text{sign}(c_3^* x_3)(c_1^* x_1)),
$$
$$
\frac{dx_3}{dt} = A_3 x_3 + b_3(\sin(\theta^2(t))(\cos(\theta^1(t)) - \sin(\theta^1(t)))),
$$
$$
\frac{d\theta^1}{dt} \equiv \omega^1,
$$
$$
\frac{d\theta^2}{dt} = \omega^2_{free} + Lc_2^* x_2.
$$

which is equal to the following system

$$
\dot{x}_2 = A_2 x_2 + b_2(\text{sign}(c_1^* x_1)(c_3^* x_3) - \text{sign}(c_3^* x_3)(c_1^* x_1)),
$$
$$
\dot{\theta}^1(t) = \omega^1,
$$
$$
\dot{\theta}^2(t) = \omega^2_{free} + L(c_3^* x_3),
$$
$$
x_3(0) = x_{03},
$$
$$
x_1 = \int_0^t \gamma_1(t - \tau) \cos(\theta^2(t))(\cos(\theta^1(t)) - \sin(\theta^1(t))) d\tau,
$$
$$
x_3 = \int_0^t \gamma_3(t - \tau) \cos(\theta^2(t))(\cos(\theta^1(t)) - \sin(\theta^1(t))) d\tau
$$

(36)

Denote

$$f_{QPSK}(\theta^1, \theta^2) = b_2(\text{sign}(c_1^* x_1)(c_3^* x_3) - \text{sign}(c_3^* x_3)(c_1^* x_1))$$

$$x_1 = \int_0^t \gamma_1(t - \tau) \cos(\theta^2(t))(\cos(\theta^1(t)) - \sin(\theta^1(t)))d\tau,$$

$$x_3 = \int_0^t \gamma_3(t - \tau) \cos(\theta^2(t))(\cos(\theta^1(t)) - \sin(\theta^1(t)))d\tau$$

Similar to BPSK Costas loop theorem 2 gives the following estimate

$$\left| \int_{s_0}^{s_0 + \varepsilon^{\frac{1}{4}}} \left(f_{QPSK}(\omega^1 t, \theta_\Delta) - \varphi(\theta_\Delta) \right) dt \right| \leq O\left(\sqrt{\varepsilon}\right), \quad \forall s_0, \quad 1 \leq s_0 + 1 \leq T.$$

By theorem 4 solutions of the equation of QPSK Costas loop in signal space (20) and in phase space (35) are close in the following sense

$$|x(t) - z(t)| = O(\varepsilon^{\frac{1}{4}}), \quad t \in [0, T].$$

Theorem 4 gives very good estimate of the difference between solutions of the averaged and original equations (Artstein, 2007). However this theorem can not be applied for Costas loops with some other waveforms, which don't meet Lipschitz condition. There are several generalizations of theorem 4 for discontinuous systems (Samoilenko, 1963; Mitropolsky, 1967; Mossaheb, 1983; Iannelli et al., 2006). Here we will consider one of the original theorems proposed by Samoilenko A.M. This theorem doesn't give such a good estimates as theorem 4, but it is very easy to apply to the Costas loop equations because of the non-linearity form of the right-hand side.

Consider system of differential equations

$$\frac{dx}{dt} = X(t, x, \lambda), \tag{37}$$

where x, X are points of n-dimensional Euclidean space E_n, λ is a parameter.

Let function $X(t, x, \lambda)$ be real measurable function in $t \in [0, T]$, $x \in D$ for any $\lambda \in \Lambda$, $\lambda_0 \in \Lambda$, where Λ is a domain of E_n.

Theorem 5. *Consider the following system*

$$\frac{dx}{dt} = \varepsilon X(t, x). \tag{38}$$

Assume that the right-hand side $X(t, x)$ is uniformly bounded and integrals

$$\int_0^t \int_c^x X(t, x)dxdt, \quad 0 \leq t < \infty, \quad x \in D \tag{39}$$

are smooth for any fixed $c \in D$; the following limit

$$\lim_{T \to \infty} \frac{1}{T} \int_0^T X(t, x) dt = X_0(x) \tag{40}$$

is exists (uniformly with respect to $x \in D$); uniformly with respect to x, r_m

$$\lim_{T \to \infty} \frac{1}{T} \int_0^T \frac{X_\Delta(t, x_1, \ldots, x_i + r_m, \ldots, x_n) - X_\Delta(t, x)}{r_m} dt = 0,$$

$$x + r_m \in D, \tag{41}$$

where r_m is a decreasing sequence ($r_m \to 0$ while $m \to \infty$), and $X_\Delta = X(t, x) - X_0(x)$; $X_0(x)$ are k-Lipschitz functions; solution $z(t)$ of the averaged equation

$$\frac{dz}{dt} = \varepsilon X_0(z),$$

for any t from $0 \leq t < \infty$ belongs to the domain D together with its ρ-neighborhood, and solution of the (38) with initial conditions $x(0) = \xi(0)$ is unique.

Then for any $\eta > 0$, $T > 0$ there is an $\varepsilon_0 > 0$, such that for $0 < \varepsilon < \varepsilon_0$ the solution $x(t)$ of (38) satisfies

$$|x(t) - \xi(t)| < \eta, \quad t \in [0, \frac{T}{\varepsilon}] \tag{42}$$

Since only piecewise-differentiable waveforms are considered, condition (39) is satisfied. Condition (40) follows from relation

$$\lim_{T \to \infty} \frac{1}{T} \int_0^T \left(f_{BPSK}(\omega^1 t, \theta_\Delta) - \varphi(\theta_\Delta) \right) dt =$$

$$= \lim_{T \to \infty} \int_0^1 \left(f_{BPSK}(\omega^1 T \tau, \theta_\Delta) - \varphi(\theta_\Delta) \right) d\tau$$

and theorem 1 (theorem 2 for QPSK Costas loop). Since

$$\lim_{T \to \infty} \frac{1}{T} \int_0^T \left(f_{BPSK}(\omega^1 t, \theta_\Delta + r_m) - \varphi(\theta_\Delta + r_m) f_{BPSK}(\omega^1 t, \theta_\Delta) - \varphi(\theta_\Delta) \right) dt = 0$$

$$\tag{43}$$

for any $r_m \to 0$ where r_0 is a constant condition (41) is also met. So, (42) can be used to estimate the difference between solutions of differential equations in signal space and in phase space.

In this chapter we provided phase detector characteristics of QPSK Costas loop and BPSK Costas loop for variety of signal waveforms. These characteristics allowed to derive nonlinear mathematical models of Costas loops in phase space. Phase space models are described by nonlinear autonomous differential

equations. Averaging theory, described in the last section, allowed to estimate how well the models of Costas loops in phase space estimate real physical system. Derived systems are much simpler to analyse than original system of non-autonomous differential equations both with analytical and computational methods. Next section explains how to use these systems to analyse Costas loops by simulation.

3 SIMULATION

Accurate and fast numerical simulation of PLL-based systems, such as Costas loops, is of great practical importance. As mentioned in (Lai et al., 2005) direct time domain simulation of PLL-based systems at the level of SPICE (Simulation Program with Integrated Circuit Emphasis) circuits is generally inefficient: "PLL transients can last hundreds of thousands of cycles, with each cycle requiring hundreds of small timesteps for accurate simulation of the embedded voltage-controlled oscillator (VCO)". Furthermore, extracting phase of frequency information, one of the chief metrics of PLL performance, from time-domain waveforms is often difficult and inaccurate. The same is true for Costas loops.

In this section we will generalize another popular approach towards fast and accurate simulation of Costas loops in phase domain. Here we will use Matlab Simulink tool, which is became a popular software tool for designing, simulation, and investigation of PLL-based systems (see, e.g.(Lai et al., 2005; Kozak and Friedman, 2004; Hanumolu et al., 2004; Brigati et al., 2001)).

3.1 Simulation of BPSK Costas loop

3.1.1 Software model description

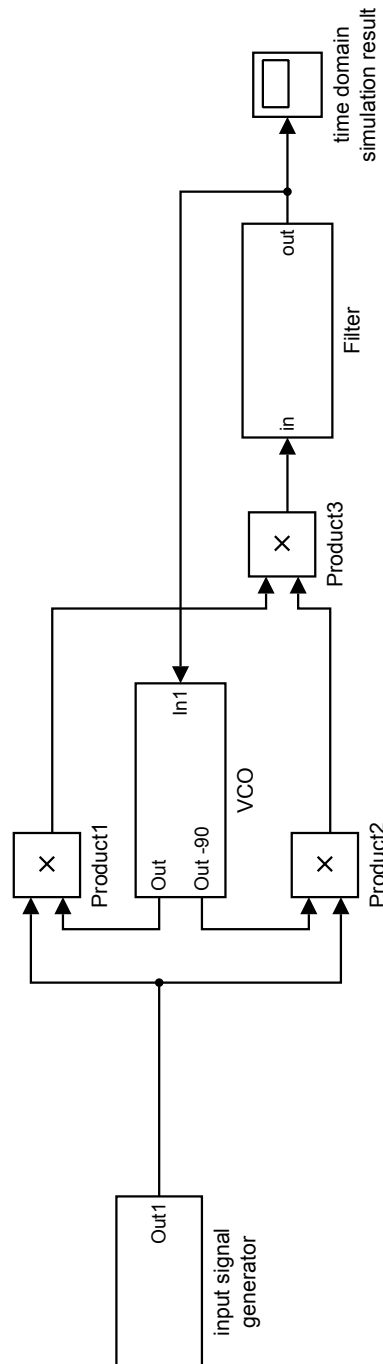Consider Matlab Simulink model of BPSK Costas loop in signal space (Fig. 7).

FIGURE 7   Software model of BPSK Costas loop in signal space

It is consist of four standard blocks and three subsystems. Standard blocks

Product1, Product2, and Product3 corresponds to the multipliers of BPSK Costas loop (see Fig. 3). Block time domain simulation result is a Scope element from standard Simulink library, which allows to plot simulation results.

Structure of the input signal generator block is shown on Fig. 8.
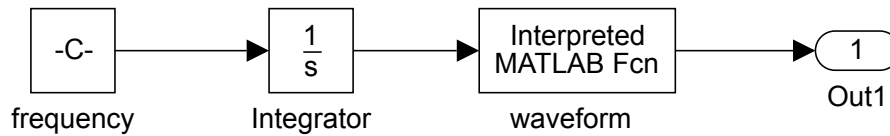

FIGURE 8   Input signal generator

This block allows to specify input signal and consists of three elements from standard library: constant block specifies the carrier frequency of the input signal, integrator reproduces phase of the carrier, and Interpreted MATLAB Fcn determines waveform of the carrier.

Internal structure of the VCO subsystem on Fig. 7 is shown on Fig. 9.
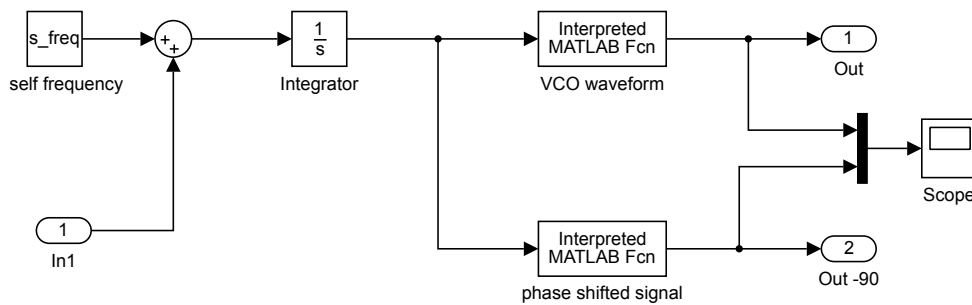
FIGURE 9   Internal structure of the VCO subsystem

VCO consists of three standard blocks: constant signal block self frequency defines VCO self (free) frequency, summing block and Integrator. VCO waveform block and phase shifted signal block determine waveform of VCO by interpreted Matlab function.

Filter subsystem from Fig. 7 is shown on Fig. 10. It is used to simulate the filter of BPSK Costas loop (Fig. 3)
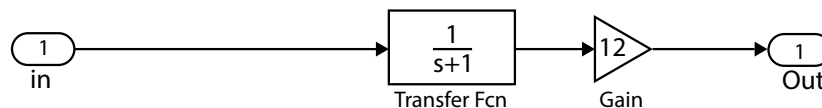

FIGURE 10   Loop filter

Filter subsystem consists of two standard blocks: block Transfer Fcn, which defines transfer function of the filter, and Gain block, which multiplies the amplitude of the filter by certain value.

Now consider Matlab Simulink model for investigation of BPSK Costas loop in phase space (Fig. 14).

Block input carrier phase is shown in Fig. 11.
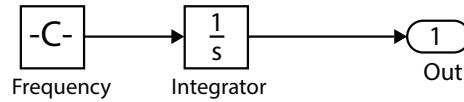

FIGURE 11   Input carrier phase subsystem

Here constant signal block Frequency determines the frequency of the input signal, and block Integrator generates phase. The structure of the block PD (Fig. 14) is shown in Fig. 12.
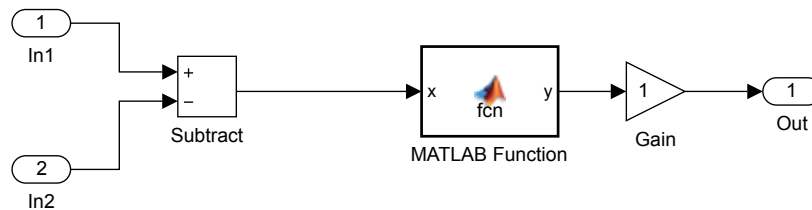
FIGURE 12   PD

Here Substract block's output is equal to the difference of the input signals. MATLAB Function allows to specify the phase detector characteristics by providing corresponding function. Gain block determines the amplitude of the output signal.

VCO subsystem is explained in Fig. 13.
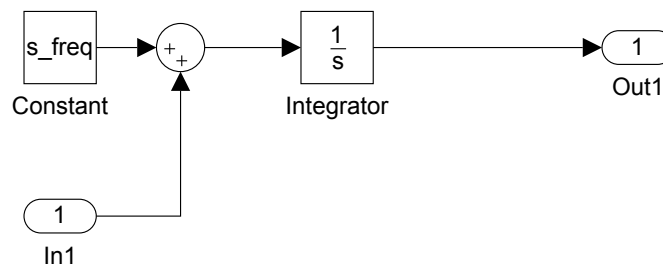
FIGURE 13   VCO subsystem structure

VCO consists of three building blocks: constant output block Constant, which determines own (free) frequency of the VCO, adder unit and Integrator. Loop Filter is the same as in Fig. 10
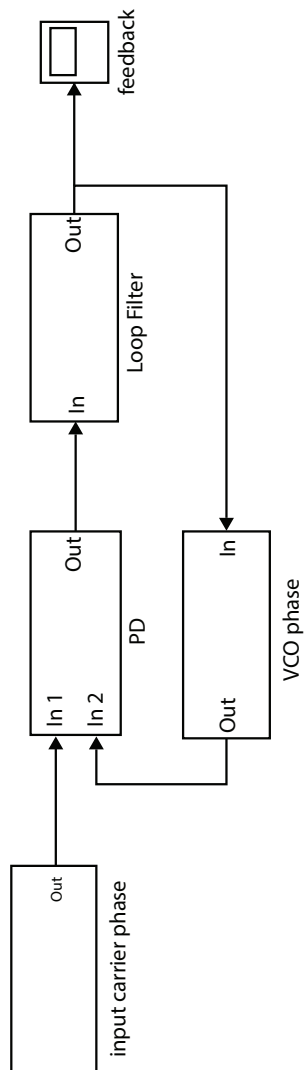
FIGURE 14   Costas loop model in phase space

For comparison of the simulation results in signal space and in phase space it is better to use hybrid model shown in Fig. 15.

FIGURE 15   Hybrid model

Described software models are versatile enough and allow to analyze vari-

ety of modifications of Costas loops, for example, with non-linear VCO, digital filters, digital VCOs, e.t.c. However, to obtain correct simulation results in the phase space, these modifications should retain the phase detector characteristics.

3.1.2 Simulation results

As noted in the introduction numerical simulation in signal space requires huge amount of computing power to study Costas loops with high frequency 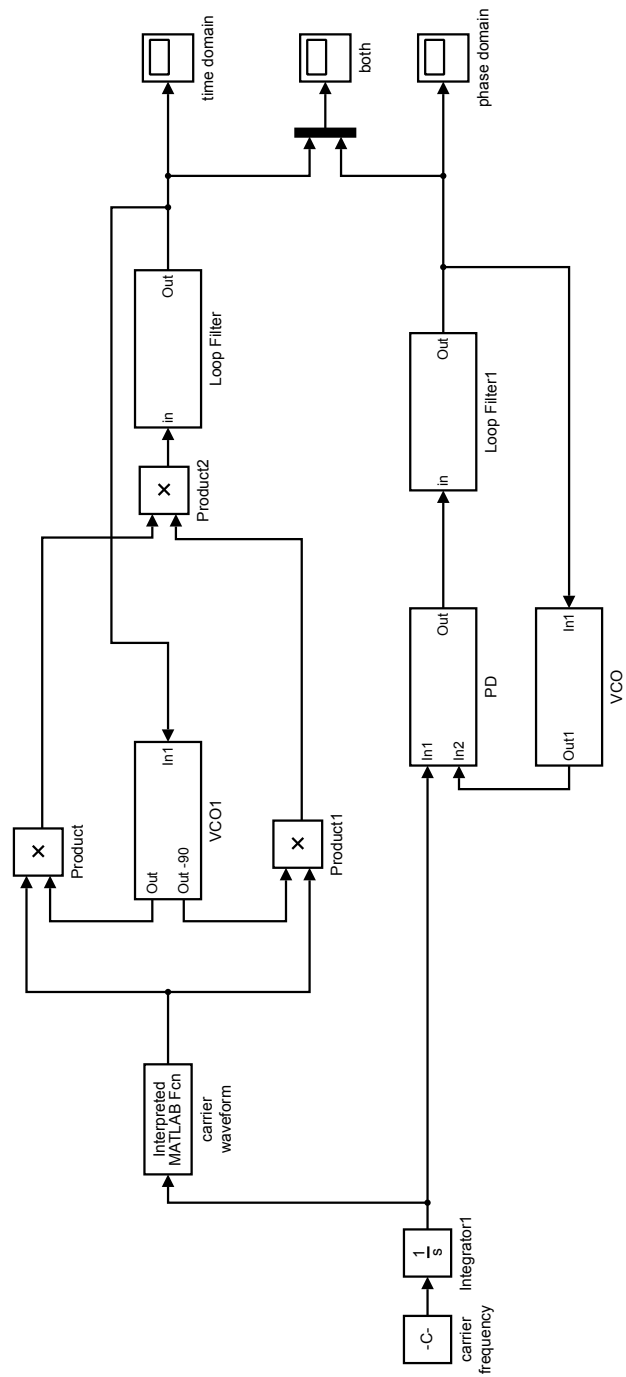signals.Therefore, a comparative analysis of transients by numerical simulations in the phase space and signal space is possible only for signals with a sufficiently low frequency.

Consider Costas loop with sawtooth VCO signal and triangular input signal carrier.

Initial conditions and parameter values are as follows: the carrier frequency of the input signal is m_freq $= 100$, Matlab function *-sawtooth(u,0.5)* gives triangular waveform for input carrier, the natural frequency of the modulating oscillator s_freq $= 101$, VCO and phase-shifted VCO waveforms are defined by Matlab functions *sawtooth(u)* and *sawtooth(u-pi/2)* correspondingly, transfer function of the filters is equal to $F(s) = \frac{1}{1+s}$, Gain value is $gain = 30$, sampling interval is $t_\Delta = 10^{-4}$, simulated period is $T = 20$. Phase detector characteristics is defined by the following function:

```
1  function y = fcn(x)
2  %#codegen
3  y = 2/pi/8*sin(2*x);
4  for i=1:1
5      l = 4*i;
6      y = y + 4/pi^2/l^4*cos(l*x);
7      l = 4*i+2;
8      y = y + 2/pi/l^3*sin(l*x);
9  end
10 y = -1/72 + y*8/pi^2;
```

The simulation results in the phase space and a signal space are shown in Fig. 16 and Fig. 17.

44
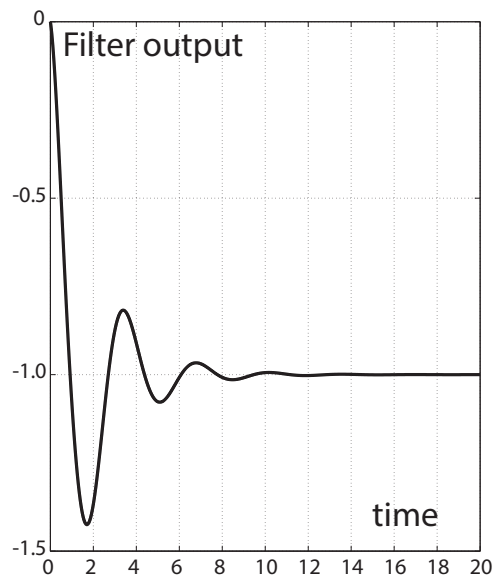
FIGURE 16   Simulation of the filter output in phase space.
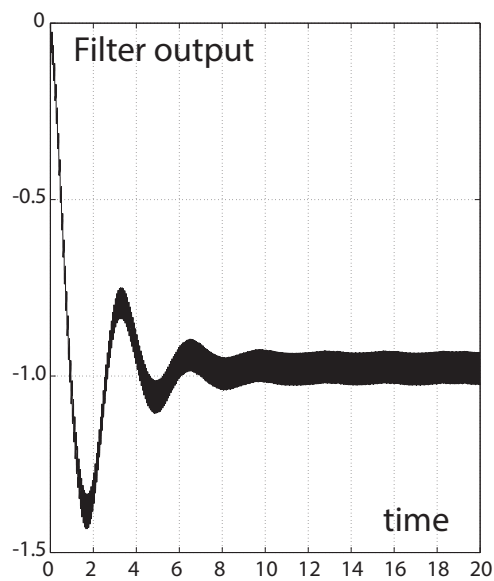
FIGURE 17   Simulation of the filter output in signal space.

In Fig. 18 both results of simulation in signal space and in phase space are shown in the same figure for the following parameters: the carrier frequency of the input signal is m_freq = 100, Matlab function *-sawtooth(u,0.5)* gives triangular waveform for input carrier, the natural frequency of the modulating oscillator s_freq = 100.5, VCO and phase-shifted VCO waveforms are defined by Matlab

functions *sawtooth(u)* and *sawtooth(u-pi/2)* correspondingly, transfer function of the filters is equal to $F(s) = \frac{1}{2+s}$, Gain value is *gain* = 27, sampling interval is $t_\Delta = 10^{-4}$, simulated period is $T = 20$.
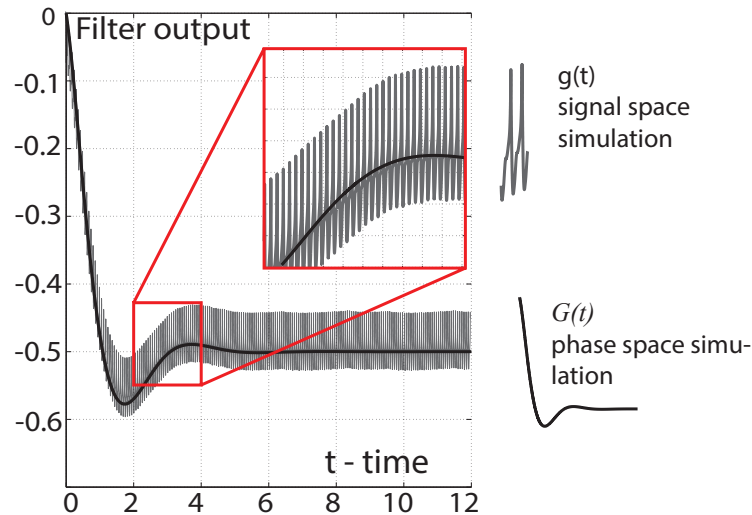
FIGURE 18   Comparison of simulation in phase space and in signal space

It is easy to see (Fig. 18) that the numerical simulation in phase space allows to reliably estimate the time of transients of Costas loop. However, simulation in phase space with the same configuration of hardware and software components [1], took almost 1000 times less time of computations (1 second versus 987 seconds).

Consider now Costas loop with triangular signals.

Initial conditions and parameter values are as follows: the carrier frequency of the input signal is m_freq = 100, Matlab function *-sawtooth(u,0.5)* gives triangular waveform for input carrier, the natural frequency of the modulating oscillator s_freq = 101, VCO and phase-shifted VCO waveforms are defined by Matlab functions *sawtooth(u),0.5* and *-sawtooth(u-pi/2,0.5)* correspondingly, transfer function of the filters is equal to $F(s) = \frac{1}{1+s}$, Gain value is *gain* = 50, sampling interval is $t_\Delta = 10^{-4}$, simulated period is $T = 20$. Phase detector characteristics is defined by the following function:

```
1  function y = fcn(x)
2  %#codegen
3  y = 0;
4  for i=0:0
5      y = y +sin((4*i+2)*x)/(4*i+2)^5;
6  end
7  y = - y*512/pi^5;
```

.

---

[1]   Intel Core I3 2100 GHz, 8Gb DDR3, Linux Ubuntu 12.10, Matlab R2013a

The simulation results in the phase space and a signal space are shown in Fig. 19 and in Fig. 20.
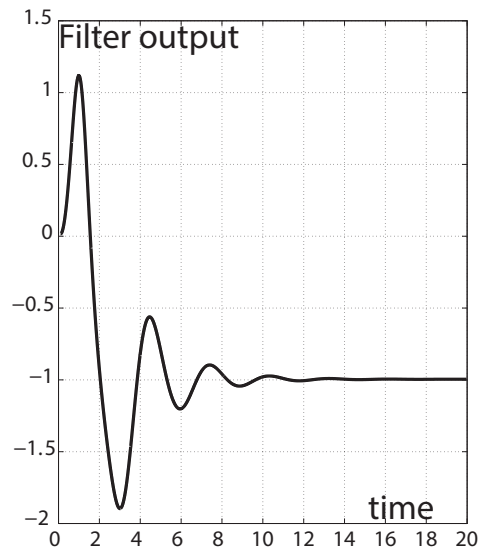

FIGURE 19   Simulation of BPSK Costas loop with triangular waveforms in phase space.
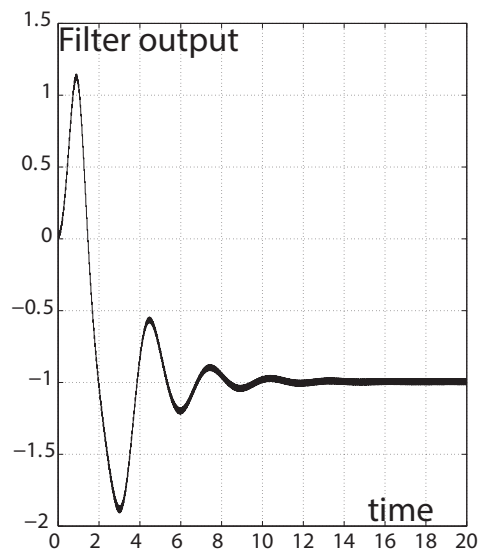

FIGURE 20   Simulation of BPSK Costas loop with triangular waveforms in signal space.

Simulation in signal space took 618 seconds and in phase space — less than a second.

Consider now Costas loop with sawtooth signals.

Initial conditions and parameter values are as follows: the carrier frequency of the input signal is m_freq $= 100$, Matlab function *-sawtooth(u,0.5)* gives triangular waveform for input carrier, the natural frequency of the modulating oscillator s_freq $= 101$, VCO and phase-shifted VCO waveforms are defined by Matlab functions *sawtooth(u)* and *-sawtooth(u-pi/2)* correspondingly, transfer function of the filters is equal to $F(s) = \frac{1}{1+s}$, Gain value is $gain = 30$, sampling interval is $t_\Delta = 10^{-4}$, simulated period is $T = 20$. Phase detector characteristics is defined by the following function:

```
function y = fcn(x)
%#codegen
y = 0;
l = 2;
y = y - 8/pi^3/l^3*sin(l*x);
l = 1;
y = y - 4*(pi*l - 2)/pi^4/l^4*cos(l*x)
      - 4*(pi*l - 2)/pi^4/l^4*sin(l*x);
l = 3;
y = y + 4*(pi*l + 2)/pi^4/l^4*cos(l*x)
      - 4*(pi*l + 2)/pi^4/l^4*sin(l*x);
for i=1:5
    l = 4*i;
    y = y + 16/pi^4/l^4*cos(l*x);
    l = 4*i + 2;
    y = y - 8/pi^3/l^3*sin(l*x);
    l = 4*i + 1;
    y = y - 4*(pi*l - 2)/pi^4/l^4*cos(l*x)
          - 4*(pi*l - 2)/pi^4/l^4*sin(l*x);
    l = 4*i + 3;
    y = y + 4*(pi*l + 2)/pi^4/l^4*cos(l*x)
          - 4*(pi*l + 2)/pi^4/l^4*sin(l*x);
end
y = y/2;
y = y - 1/72;
```

The simulation results in the phase space and a signal space are shown in Fig. 21 and in Fig. 22.
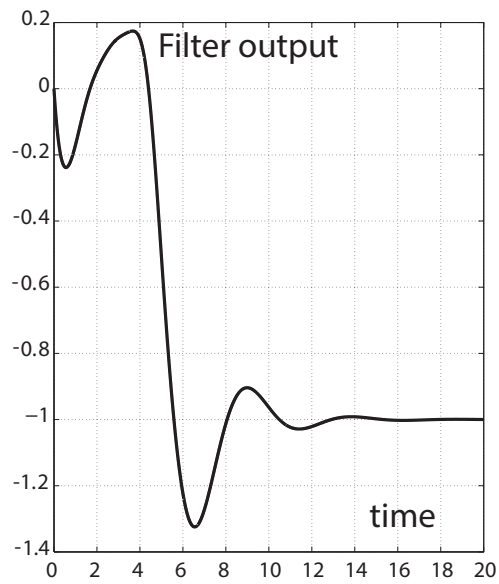
FIGURE 21   Simulation of BPSK Costas loop with sawtooth waveforms in phase space.
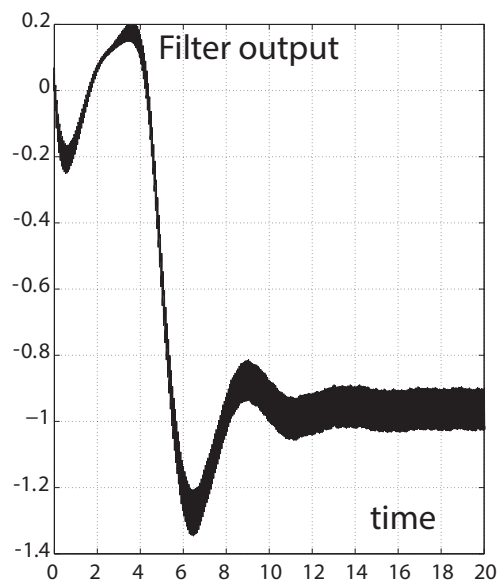
FIGURE 22   Simulation of BPSK Costas loop with sawtooth waveforms in signal space.

Simulation in signal space took 493 seconds and in phase space — less than a second.

Consider Costas loop with triangular VCO signal and sawtooth input signal carrier.

Initial conditions and parameter values are as follows: the carrier frequency of the input signal is m_freq $= 100$, Matlab function -*sawtooth(u)* gives triangular waveform for input carrier, the natural frequency of the modulating oscillator s_freq $= 101$, VCO and phase-shifted VCO waveforms are defined by Matlab functions *sawtooth(u,0.5)* and *sawtooth(u-pi/2,0.5)* correspondingly, transfer function of the filters is equal to $F(s) = \frac{1}{1+s}$, Gain value is $gain = 100$, sampling interval is $t_\Delta = 10^{-4}$, simulated period is $T = 20$. Phase detector characteristics is defined by the following function:

```
1  function y = fcn(x)
2  %#codegen
3  y = 0;
4  for i=0:0
5      y = y +sin((4*i+2)*x)/(4*i+2)^5;
6  end
7  y = y*128/pi^5;
```

The simulation results in the phase space and a signal space are shown in Fig. 23 and in Fig. 24.
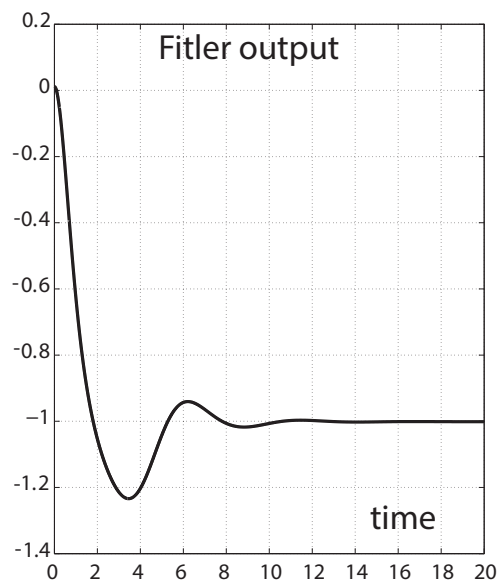
FIGURE 23   Sawtooth and triangular waveforms. Phase space.
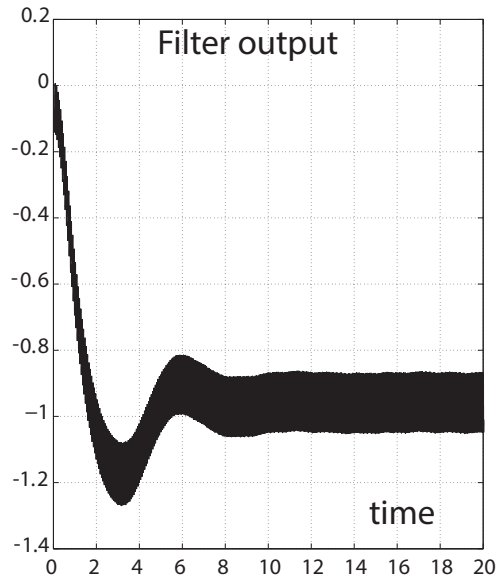
FIGURE 24   Sawtooth and triangular waveforms. Signal space.

Simulation in signal space took 493 seconds and in phase space — less than a second.

3.1.3 Simulation of digital circuits

The derived method can be adapted for the numerical simulation of the digital Costas loops. The main idea is to select an analog filter with appropriate characteristics. For example analog filter with transfer function $\frac{1}{0.1s+1}$ corresponds to digital filter $\frac{10}{1-\exp^{-10T}z^{-1}}$, where T is discretization step (sample time) [2].

Simulink model of digital filter is shown in Fig. 25,
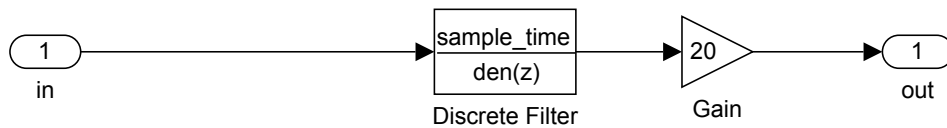
FIGURE 25   Digital filter

where set of parameters of Discrete filter are show in Fig. 26.

---

[2]   The process for selecting the appropriate filters by their characteristics in general case is described in (Thede, 2005).
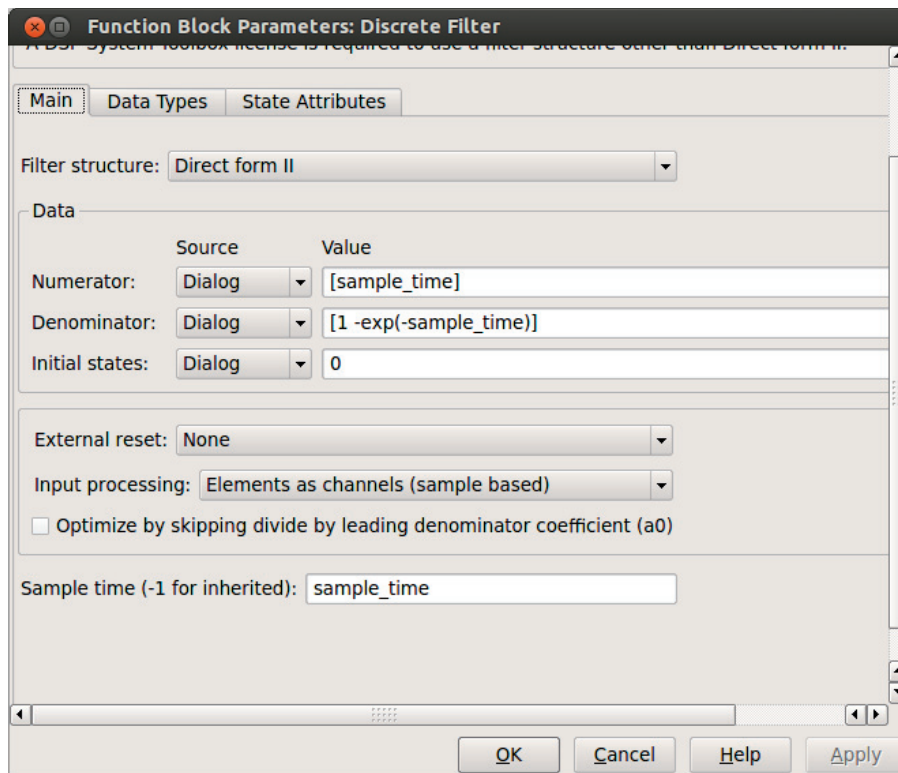
FIGURE 26   Digital filter parameters

Fig. 27 shows the results of simulation of digital Costas loop in phase space and a in signal space for the sawtooth input carrier signal waveform and triangular VCO signal with the following parameters: VCO self (free) frequency — 105 Hz, carrier frequency — 100 Hz, Gain $= 100$, transfer function of analog filter $F(s) = \frac{1}{0.1s+1}$, digital filter characteristics $F(z) = \frac{10}{1-\exp^{-10T} z^{-1}}$, sample time $T = 10^{-3}$.
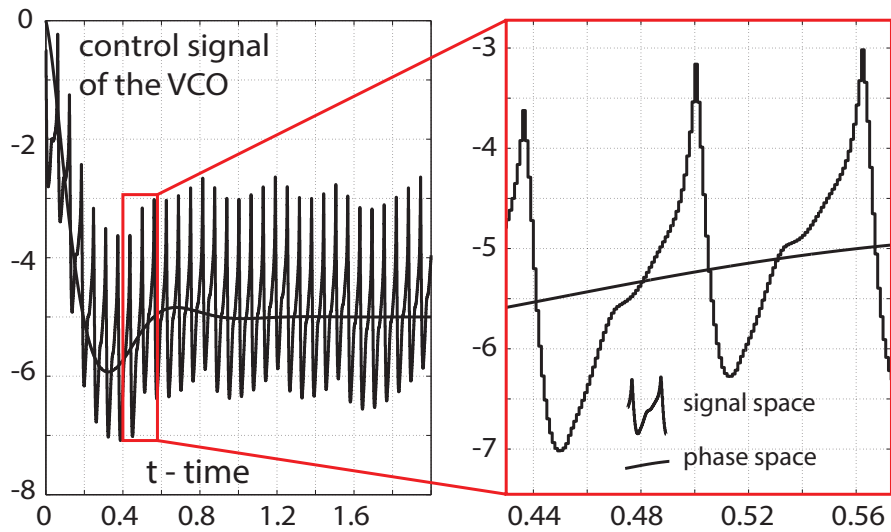
FIGURE 27   Simulation of digital Costas loop

3.2   Simulation of QPSK Costas loop

In the first chapter it has been shown that the mathematical model of QPSK Costas loop in phase space coincides with the model of BPSK Costas loop. The only difference is phase detector characteristics. Consider the Simulink model of QPSK Costas in signal space (Fig. 29). Here we have two custom blocks — input carrier signal and VCO. Internals of input carrier signal are shown in Fig. 28.
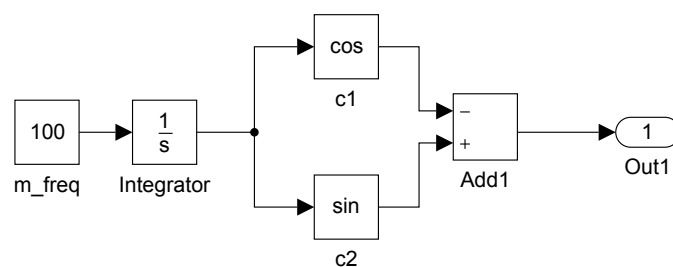
FIGURE 28   Input carrier signal

Here block constant signal block m_freq determines the frequency of the input signal, and Integrator generates phase. Then blocks c1 and c2 are form two carrier signals.

VCO subsystem internals are shown in Fig. 30.
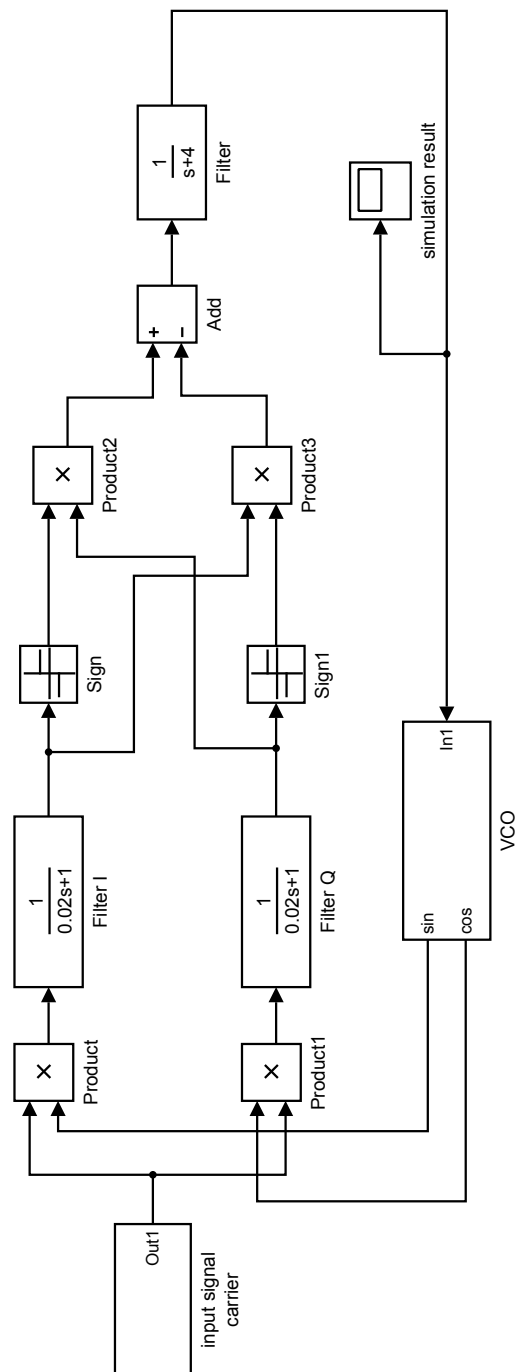
FIGURE 29   QPSK Costas loop model. Signal space.
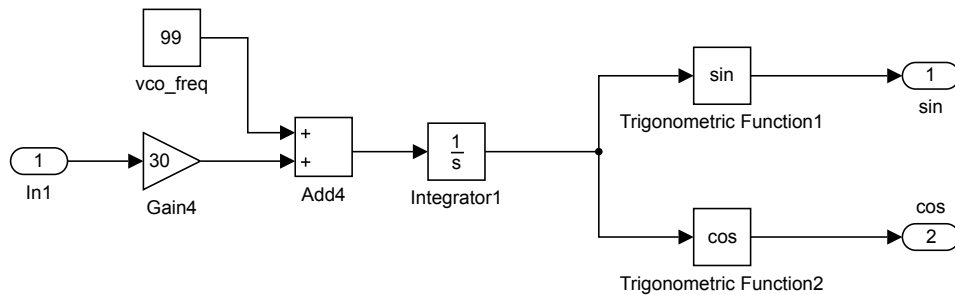
FIGURE 30   VCO subsystem

It is consist of the following standard library blocks: constant signal block vco_freq,stroke which determines self frequency of VCO, Integrator block, summing block, Gain, and two blocks which defines sinusoidal waveforms.

Results of simulation of QPSK Costas loop are shown in Fig. 31 in signal space and in phase space.
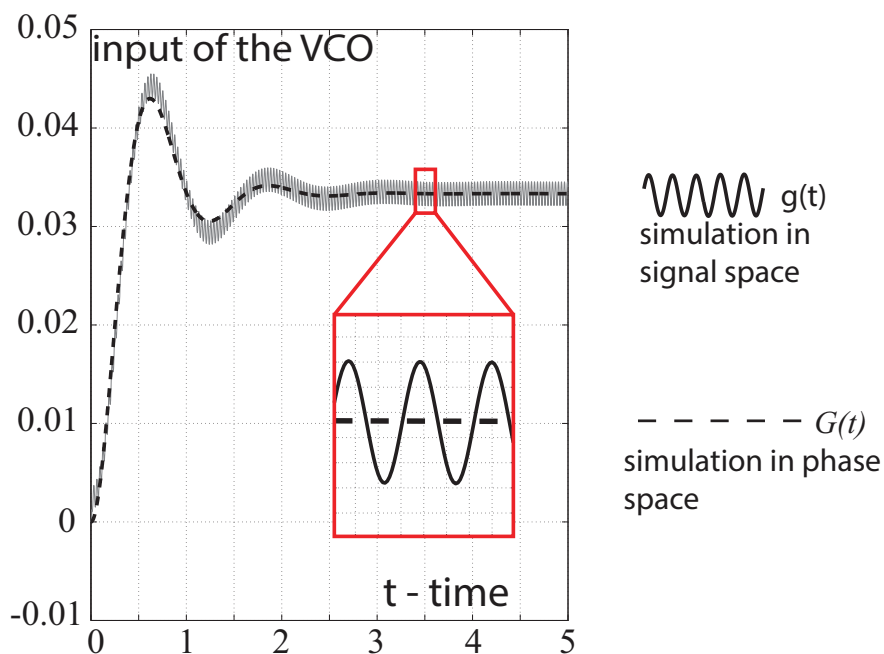
FIGURE 31   Simulation of QPSK Costas loop in phase space and in signal space

Parameters values are as follows: phase detector characteristics is defined by the following MATHAL function:

```
1  function y = fcn(u)
2  %#codegen
```

```
3  y = -0.5*sqrt(2)*(sin(u + pi/4)*sign(sin(u - pi/4)));
4  y = y + 0.5*sqrt(2)*(sin(u - pi/4)*sign(sin(u + pi/4)));
5  end
```

Input carrier frequency is equal to m_freq = 100, VCO free frequency is s_freq = 99, filter 2 transfer function is $F(s) = \frac{1}{4+s}$, Filter 1 and filter 3 transfer functions are $F(s) = \frac{1}{1+0.02s}$, $Gain = 30$, discretization step is $t_\Delta = 10^{-4}$, simulated time period is equal to $T = 5$.

3.3 Frequency of the signals and accuracy of simulation

In modern Costas loop-based devices the frequencies of VCO and input carrier can be very high(up to 85–87 GHz (Huang et al., 2011)). Therefore it is important to determine how the increase in frequency affects simulation process.

Accuracy of simulation behaves similarly for all waveforms. Consider the simulation of Costas loop with sawtooth VCO signal and triangular input carrier signal.

The parameters and the initial data other than the frequency and sampling step, will be the same as before: sawtooth input carrier waveform is defined by Matlab function -sawtooth(u,0.5), triangular VCO signal is defined by function sawtooth(u), analog filter transfer function $F(s) = \frac{1}{1+s}$, $gain = 30$. Simulation results are shown in the following table, where m_freq is frequency of input carrier, s_freq is frequency of VCO, and discretization step is equal to t_Δ. Difference between simulation in phase space and in signal space is marked by red colour.

$m\_freq = 50 Hz,$
$s\_freq = 51 Hz,$
$t_\Delta = 0.0002$

$m\_freq = 100 Hz,$
$s\_freq = 101 Hz,$
$t_\Delta = 0.0001$
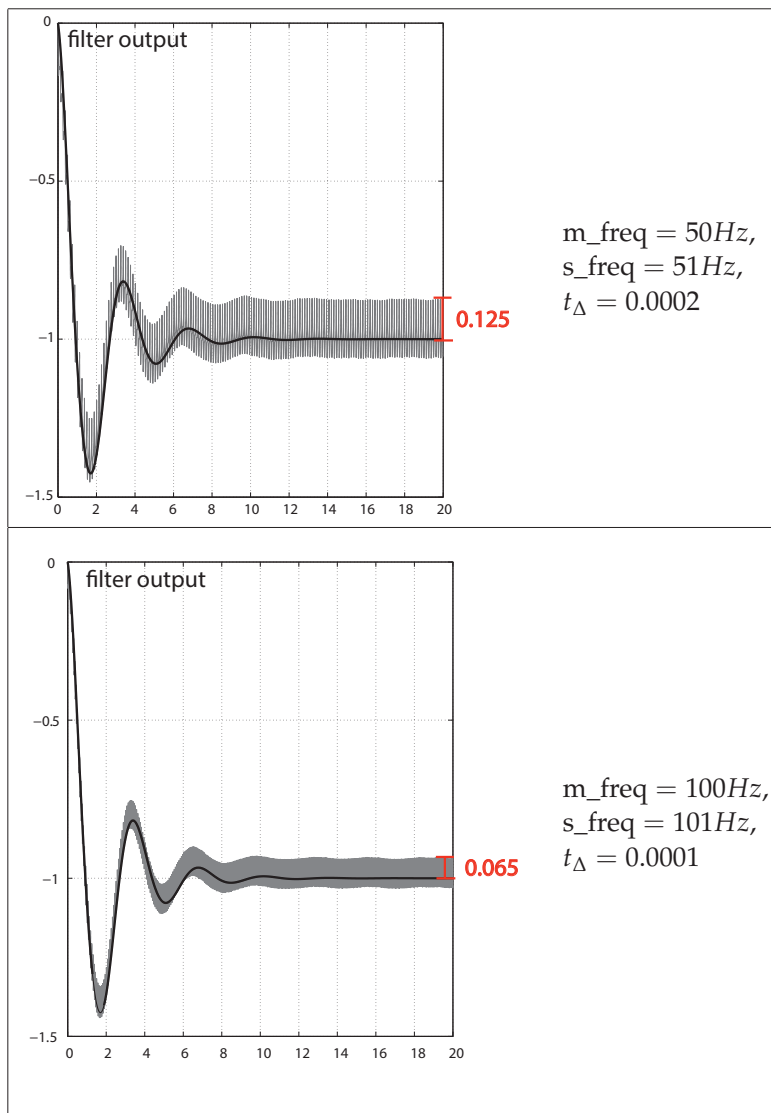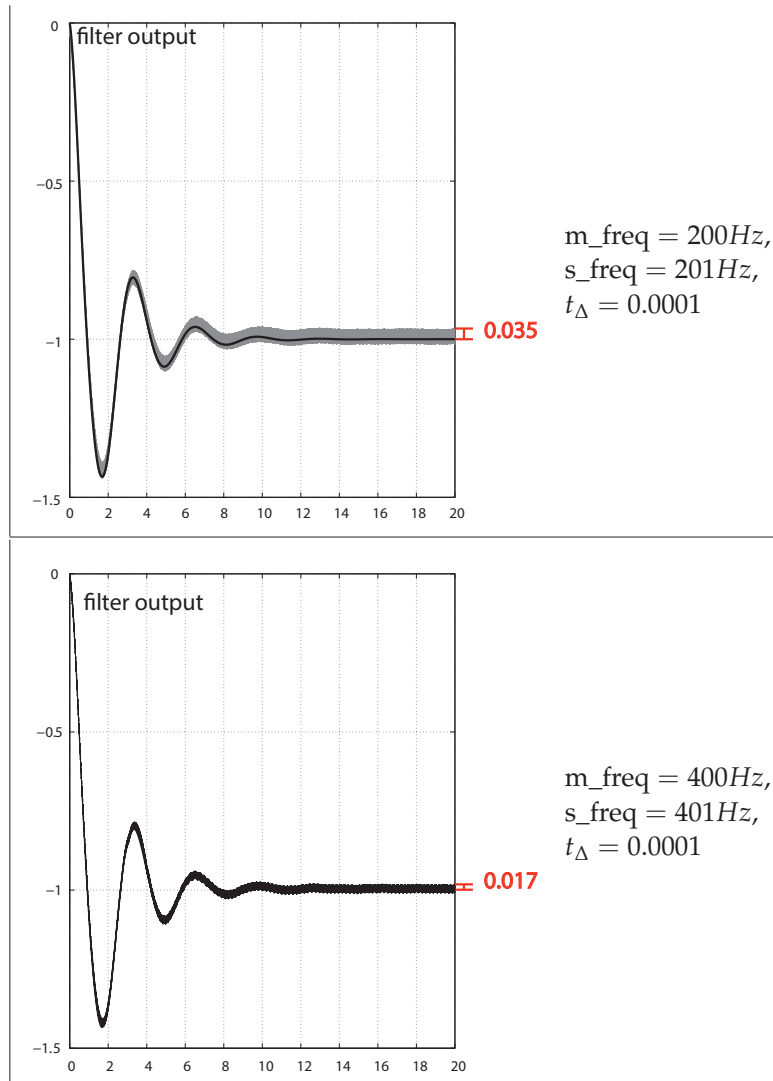
It is easy to see, that experimental results are consistent with theoretical estimations. As we can see convergence rate is almost linear, which is even faster than square root[3] mentioned in theorem 1. This is due to the stable filter with smooth and exponentially decreasing impulse response function and continuous input signal carrier waveform.

The efficiency of the proposed method is confirmed by the numerical simulation of the Costas loop for high-frequency signals. In Fig. 32, an example of modelling the classic Costas loop with 1Ghz signals is shown[4].

---

[3] $\qquad O(\delta) = O(\frac{1}{\sqrt{\omega}_{min}})$

[4] $\qquad$ The parameters of simulation are the same as in 21 except the frequencies and discretization step (10^{-11}).

58
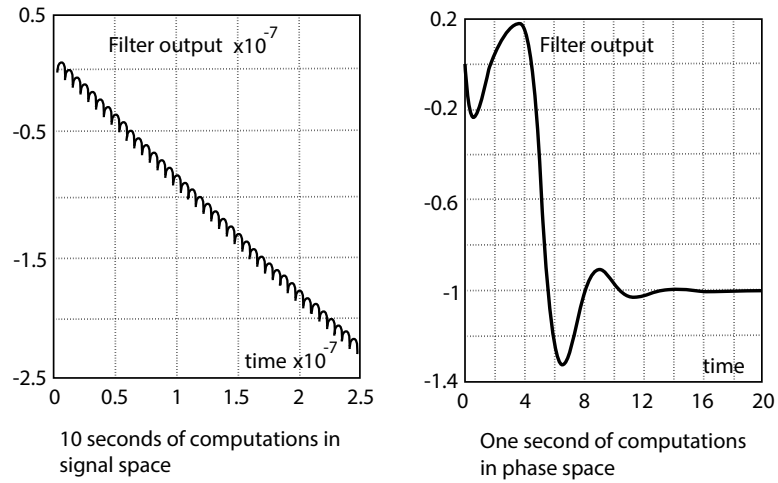
FIGURE 32   Comparison of the effectiveness of simulation in signal space and phase space

Here, in the course of 10 seconds of computing in the signal space (where the process of computation is very slow), only 2.5×10^{-7} seconds of the transient processes have been modeled. Therefore, the numerical simulation of the full transient process in the signal space is almost impossible for high-frequency signals. At the same time, the full simulation time of 20 seconds of the transient processes in the phase space took less than a second.

4 CONCLUSION

First chapter provided reasoning for investigation of Costas loops and stated the main problems. In the second chapter we derived nonlinear mathematical models of BPSK Costas loop and QPSK Costas loop for variety of signal waveforms. The averaging methods allowed to justify that the solutions of differential equations in the phase space are close to the solutions in the signal/time space. Derived systems are much simpler to analyse than original system of non-autonomous differential equations both with analytical and computational methods. Third chapter showed that proposed models can be effectively used to investigate important Costas loop characteristics and significantly reduce simulation time. Simulation speed-up allowed to analyse transient processes in reasonable time that wasn't possible for some Costas loops. Finnish patent application was filled based on results obtained in this thesis.

60

YHTEENVETO (FINNISH SUMMARY)

Työssä tarkastellaan ns Costas loop-piirien matemaattisia malleja. Costas loop-piirit keksi John P. Costas General Electric-yhtiöstä v. 1956. Tätä nykyä Costas loop-piiri on laajassa käytössä erilaisissa sovelluksissa, muun muassa tietoliiken-nejärjestelmissä, GPS-järjestelmissä, lääketieteellisissä implanteissa ja muissa lait-teissa.

Costas loop-piiri perustuu vaihelukittuun piiriin (phase-locked loop, PLL) ja sillä on kaksi erillistä tehtävää: kantoaallon uudelleen aktivointi ja tietojen demodulointi. Costas loop on siksi monimutkaisempi kuin PLL-piiri sisältäen kolme epälineaarista elementtiä yhden sijasta. Tämä vaikeuttaa piirien analyyt-tista tarkastelua. Costas loop -piirien suora simulointi ei ole mielekästä nykyaikai-sissa laitteissa käytettävien korkeiden taajuuksien takia.

Tässä työssä on kehitetty epälineaarisia matemaattisia malleja Binary Phase Shift Keying (BPSK) Costas loop-piirien ja Quadrature Phase Shift Keying (QPSK) Costas loop-piirien analysointiin taajuustasossa .

Mallit helpottavat analyyttisten menetelmien soveltamista ja lyhentävät oleel-lisesti numeerisen simuloinnin aikaa. Mallien asymptoottista tarkkuutta korkeataa-juisille signaaleille on tarkasteltu sekä teoreettisesti että kokeellisesti erilaisille käytännössä tarvittaville aaltomuodoille.

REFERENCES

Abe, T., Yuan, Y., Ishikuro, H. & Kuroda, T. 2012. A 2gb/s 150mw uwb direct-conversion coherent transceiver with iq-switching carrier recovery scheme. In Solid-State Circuits Conference Digest of Technical Papers (ISSCC), 2012 IEEE International, 442–444.

Abramovitch, D. 2002. Phase-locked loops: A control centric tutorial. In Proceedings of the American Control Conference, Vol. 1, 1–15.

Abramovitch, D. 2008a. Efficient and flexible simulation of phase locked loops, part II: post processing and a design example. In American Control Conference. Seattle, WA: , 4678–4683.

Abramovitch, D. 2008b. Efficient and flexible simulation of phase locked loops, part I: simulator design. In American Control Conference. Seattle, WA: , 4672–4677.

Agbinya, J. I. 2011. Principles of Inductive Near Field Communications for Internet of Things, Vol. 18. River Publishers.

An'an, Z. & Du Yong, H. F. 2006. Design and implementation of costas loop on fpga platform. Electronic Engineer 1, 18–20.

Andrievsky, B. R., Kuznetsov, N. V., Leonov, G. A. & Pogromsky, A. Y. 2012. Convergence based anti-windup design method and its application to flight control. In International Congress on Ultra Modern Telecommunications and Control Systems and Workshops. IEEE, 212–218 (art. no. 6459667). doi:10.1109/ICUMT.2012.6459667.

Artstein, Z. 2007. Averaging of time-varying differential equations revisited. Journal of Differential Equations 243 (2), 146–167.

Banerjee, T. & Sarkar, B. 2008a. Chaos and bifurcation in a third-order digital phase-locked loop. International Journal of Electronics and Communications 62, 86–91.

Banerjee, T. & Sarkar, B. C. 2008b. Chaos and bifurcation in a third-order digital phase-locked loop. International Journal of Electronics and Communications 62, 86–91.

Beier, W. 1987. Receiver for bandspread signals. (US Patent 4,672,629).

Benarjee, D. 2006. PLL Perforfmance, Simulation, and Design. Dog Ear Publishing.

Best, R. E. 2007. Phase-Lock Loops: Design, Simulation and Application. McGraw-Hill.

Bouaricha, A. et al. 2012. Hybrid time and frequency solution for PLL sub-block simulation. (US Patent 8,209,154).

Braasch, M. S. & Van Dierendonck, A. 1999. Gps receiver architectures and measurements. Proceedings of the IEEE 87 (1), 48–64.

Bragin, V. O., Kuznetsov, N. V. & Leonov, G. A. 2010. Algorithm for counterexamples construction for Aizerman's and Kalman's conjectures. IFAC Proceedings Volumes (IFAC-PapersOnline) 4 (1), 24–28. doi:10.3182/20100826-3-TR-4016.00008.

Bragin, V. O., Vagaitsev, V. I., Kuznetsov, N. V. & Leonov, G. A. 2011. Algorithms for finding hidden oscillations in nonlinear systems. The Aizerman and Kalman conjectures and Chua's circuits. Journal of Computer and Systems Sciences International 50 (4), 511-543. doi:10.1134/S106423071104006X.

Brigati, S., Francesconi, F., Malvasi, A., Pesucci, A. & Poletti, M. 2001. Modeling of fractional-n division frequency synthesizers with simulink and matlab. In Electronics, Circuits and Systems, 2001. ICECS 2001. The 8th IEEE International Conference on, Vol. 2. IEEE, 1081–1084.

Chang, G. & Chen, C. 2008. A comparative study of voltage flicker envelope estimation methods. In Power and Energy Society General Meeting - Conversion and Delivery of Electrical Energy in the 21st Century, 1–6.

Chen, H., Cao, Z. & Ge, Q. J. 2012. NOISE REGULATED LINEAR VOLTAGE CONTROLLED OSCILLATOR. (US Patent 20,120,223,781).

Chen, R., Guan, J. & Zhang, X. 2010. Design and implementation of digital costas-loop. Radio Engineering.

Chicone, C. & Heitzman, M. T. 2013. Phase-locked loops, demodulation, and averaging approximation time-scale extensions. SIAM Journal on Applied Dynamical Systems 12 (2), 674–721.

Cho, P. S. 2006. Optical phase-locked loop performance in homodyne detection using pulsed and cw lo. In Optical Amplifiers and Their Applications/Coherent Optical Technologies and Applications. Optical Society of America, JWB24.

Costas, J. 1956. Synchoronous communications. In Proc. IRE, Vol. 44, 1713–1718.

Costas, J. P. 1962. Receiver for communication system. (US Patent 3,047,659).

Couch, L. 2007. Digital and Analog Communication Systems. Pearson/Prentice Hall.

Demir, A., Mehrotra, A. & Roychowdhury, J. 2000a. Phase noise in oscillators: a unifying theory and numerical methods for characterization. IEEE Transactions on Circuits and Systems I 47, 655–674.

Demir, A., Mehrotra, A. & Roychowdhury, J. 2000b. Phase noise in oscillators: a unifying theory and numerical methods for characterization. IEEE Transactions on Circuits and Systems I 47, 655–674.

Djordjevic, I. B., Stefanovic, M. C., Ilic, S. S. & Djordjevic, G. T. 1998. An example of a hybrid system: Coherent optical system with Costas loop in receiver-system for transmission in baseband. J. Lightwave Technol. 16 (2), 177.

Djordjevic, I. B. & Stefanovic, M. C. 1999. Performance of optical heterodyne psk systems with Costas loop in multichannel environment for nonlinear second-order PLL model. J. Lightwave Technol. 17 (12), 2470.

Egan, W. F. 2000. Frequency synthesis by phase lock. Wiley New York.

Emura, T. 1982. A study of a servomechanism for nc machines using 90 degrees phase difference method. Prog. Rep. of JSPE, 419-421.

Feely, O., Curran, P. F. & Bi, C. 2012. Dynamics of charge-pump phase-locked loops. International Journal of Circuit Theory and Applications. doi:10.1002/cta.

Feely, O. 2007. Nonlinear dynamics of discrete-time circuits: A survey. International Journal of Circuit Theory and Applications 35, 515–531.

Fines, P. & Aghvami, A. 1991. Fully digital m-ary psk and m-ary qam demodulators for land mobile satellite communications. IEEE Electronics and Communication Engineering Journal 3 (6), 291–298.

Fiocchi, C., Maloberti, F. & Torelli, G. 1992. A sigma-delta based pll for non-sinusoidal waveforms. In Circuits and Systems, 1992. ISCAS '92. Proceedings., 1992 IEEE International Symposium on, Vol. 6, 2661-2664 vol.6. doi: 10.1109/ISCAS.1992.230673.

Gao, W. & Feher, K. 1996. All-digital reverse modulation architecture based carrier recovery implementation for gmsk and compatible fqpsk. Broadcasting, IEEE Transactions on 42 (1), 55–62.

Gardner, F., Erup, L. & Harris, R. 1993. Interpolation in digital modems - part II: Implementation and performance. IEEE Electronics and Communication Engineering Journal 41 (6), 998-1008.

Gardner, F. 1966. Phase–lock techniques. New York: John Wiley.

Gardner, F. 1993. Interpolation in digital modems - part I: Fundamentals. IEEE Electronics and Communication Engineering Journal 41 (3), 501–507.

Hanumolu, P. K., Brownlee, M., Mayaram, K. & Moon, U.-K. 2004. Analysis of charge-pump phase-locked loops. Circuits and Systems I: Regular Papers, IEEE Transactions on 51 (9), 1665–1674.

64

Hayami, Y., Imai, F. & Iwashita, K. 2008. Linewidth investigation for costas loop phase-diversity homodyne detection in digital coherent detection system. In Asia Optical Fiber Communication and Optoelectronic Exposition and Conference. Optical Society of America, SaK20.

Hegarty, C. J. 2012. Gnss signals - an overview. In Frequency Control Symposium (FCS), 2012 IEEE International, 1–7.

Henning, F. H. 1981. Nonsinusoidal Waves for Radar and Radio Communication (First edition). Academic Press, 396.

Hodgkinson, T. 1986. Costas loop analysis for coherent optical receivers. Electronics letters 22 (7), 394–396.

Hu, Y. & Sawan, M. 2005. A fully integrated low-power bpsk demodulator for implantable medical devices. Circuits and Systems I: Regular Papers, IEEE Transactions on 52 (12), 2552–2562.

Huang, S.-J., Yeh, Y.-C., Wang, H., Chen, P.-N. & Lee, J. 2011. W -band bpsk and qpsk transceivers with costas-loop carrier recovery in 65-nm cmos technology. Solid-State Circuits, IEEE Journal of 46 (12), 3033-3046. doi:10.1109/JSSC.2011. 2166469.

Humphreys, T. E., Psiaki, M. L., Ledvina, B. M. & Kintner Jr, P. 2005. Gps carrier tracking loop performance in the presence of ionospheric scintillations. Proceedings of ION GNSS 2005, 13–16.

Iannelli, L., Johansson, K. H., Jönsson, U. T. & Vasca, F. 2006. Averaging of nonsmooth systems using dither. Automatica 42 (4), 669–676.

Iniewski, K. 2008. VLSI circuits for biomedical applications. Artech House.

Jasper, S. C. 1987. Method of doppler searching in a digital GPS receiver. (US Patent 4,701,934).

Kanwal, N., Hurskainen, H. & Nurmi, J. 2010. Vector tracking loop design for degraded signal environment. In Ubiquitous Positioning Indoor Navigation and Location Based Service (UPINLBS), 2010. IEEE, 1–4.

Kaplan, E. & Hegarty, C. 2006. Understanding GPS: Principles and Applications. Artech House.

Kim, H., Kang, S., Chang, J.-H., Choi, J.-H., Chung, H., Heo, J., Bae, J.-D., Choo, W. & Park, B.-h. 2010. A multi-standard multi-band tuner for mobile TV SoC with GSM interoperability. In Radio Frequency Integrated Circuits Symposium (RFIC), 2010. IEEE, 189–192.

Kiseleva, M. A., Kuznetsov, N. V., Leonov, G. A. & Neittaanmäki, P. 2012. Drilling systems failures and hidden oscillations. In IEEE 4th International Conference on Nonlinear Science and Complexity, NSC 2012 - Proceedings, 109–112. doi: 10.1109/NSC.2012.6304736.

Kiseleva, M. A., Kuznetsov, N. V., Leonov, G. A. & Neittaanmäki, P. 2014. Discontinuity and Complexity in Nonlinear Physical Systems, Vol. 6. Springer. doi:10.1007/978-3-319-01411-1_15.

Kobayashi, K., Matsumoto, Y., Seki, K. & Kato, S. 1992. A full digital modem for offset type modulation schemes. In Personal, Indoor and Mobile Radio Communications, 1992. Proceedings, PIMRC'92., Third IEEE International Symposium on, 596–599.

Kozak, M. & Friedman, E. G. 2004. Design and simulation of fractional-n pll frequency synthesizers. In Circuits and Systems, 2004. ISCAS'04. Proceedings of the 2004 International Symposium on, Vol. 4. IEEE, IV–780.

Kroupa, V. 2003. Phase Lock Loops and Frequency Synthesis. John Wiley & Sons.

Krylov, N. & Bogolyubov, N. 1947. Introduction to non-linear mechanics. Princeton: Princeton Univ. Press.

Kudrewicz, J. & Wasowicz, S. 2007. Equations of phase-locked loop. Dynamics on circle, torus and cylinder, Vol. 59. World Scientific. A.

Kuznetsov, N., Kuznetsova, O., Leonov, G. & Vagaitsev, V. 2013. Informatics in Control, Automation and Robotics, Lecture Notes in Electrical Engineering, Volume 174, Part 4. doi:10.1007/978-3-642-31353-0_11.

Kuznetsov, N. V., Kuznetsova, O. A., Leonov, G. A. & Vagaytsev, V. I. 2011. Hidden attractor in Chua's circuits. ICINCO 2011 - Proceedings of the 8th International Conference on Informatics in Control, Automation and Robotics 1, 279–283. doi:10.5220/0003530702790283.

Kuznetsov, N. V., Leonov, G. A., Seledzhi, S. M. & Neittaanmäki, P. 2009a. Analysis and design of computer architecture circuits with controllable delay line. ICINCO 2009 - 6th International Conference on Informatics in Control, Automation and Robotics, Proceedings 3 SPSMC, 221–224. doi:10.5220/0002205002210224.

Kuznetsov, N. V., Leonov, G. A. & Seledzhi, S. M. 2009b. Nonlinear analysis of the Costas loop and phase-locked loop with squarer. In Proceedings of the IASTED International Conference on Signal and Image Processing, SIP 2009, 1–7.

Kuznetsov, N. V., Leonov, G. A. & Seledzhi, S. M. 2011. Hidden oscillations in nonlinear control systems. IFAC Proceedings Volumes (IFAC-PapersOnline) 18 (1), 2506–2510. doi:10.3182/20110828-6-IT-1002.03316.

Kuznetsov, N. V., Leonov, G. A. & Seledzhi, S. S. 2008. Phase locked loops design and analysis. In ICINCO 2008 - 5th International Conference on Informatics in Control, Automation and Robotics, Proceedings, Vol. SPSMC, 114–118. doi:10.5220/0001485401140118.

Kuznetsov, N. V., Leonov, G. A. & Vagaitsev, V. I. 2010. Analytical-numerical method for attractor localization of generalized Chua's system. IFAC Proceedings Volumes (IFAC-PapersOnline) 4 (1), 29–33. doi:10.3182/20100826-3-TR-4016.00009.

Kuznetsov, N. V. & Leonov, G. A. 2001. Counterexample of Perron in the discrete case. Izv. RAEN, Diff. Uravn. 5, 71.

Kuznetsov, N. V. & Leonov, G. A. 2005. On stability by the first approximation for discrete systems. 2005 International Conference on Physics and Control, PhysCon 2005 Proceedings Volume 2005, 596-599. doi:10.1109/PHYCON.2005.1514053.

Kuznetsov, N. V. & Leonov, G. A. 2008. Lyapunov quantities, limit cycles and strange behavior of trajectories in two-dimensional quadratic systems. Journal of Vibroengineering 10 (4), 460-467.

Kuznetsov, N. V., Vagaytsev, V. I., Leonov, G. A. & Seledzhi, S. M. 2011. Localization of hidden attractors in smooth Chua's systems. International Conference on Applied and Computational Mathematics, 26–33.

Kuznetsov, N. V. 2008. Stability and Oscillations of Dynamical Systems: Theory and Applications. Jyvaskyla University Printing House.

Lai, X., Wan, Y. & Roychowdhury, J. 2005. Fast pll simulation using nonlinear vco macromodels for accurate prediction of jitter and cycle-slipping due to loop non-idealities and supply noise. Proceedings of the 2005 Asia and South Pacific Design Automation Conference, 459–464.

Leonov, G. & Seledzhi, S. 2002. The Phase-Locked Loop for Array Processors. St.Petersburg [in Russian]: Nevskii dialect.

Leonov, G. A., Bragin, V. O. & Kuznetsov, N. V. 2010a. Algorithm for constructing counterexamples to the Kalman problem. Doklady Mathematics 82 (1), 540–542. doi:10.1134/S1064562410040101.

Leonov, G. A., Bragin, V. O. & Kuznetsov, N. V. 2010b. On problems of Aizerman and Kalman. Vestnik St. Petersburg University. Mathematics 43 (3), 148–162. doi:10.3103/S1063454110030052.

Leonov, G. A., Kuznetsov, N. V. & Kudryashova, E. V. 2011a. A direct method for calculating Lyapunov quantities of two-dimensional dynamical systems. Proceedings of the Steklov Institute of Mathematics 272 (Suppl. 1), S119-S127. doi:10.1134/S008154381102009X.

Leonov, G. A., Kuznetsov, N. V., Kuznetsova, O. A., Seledzhi, S. M. & Vagaitsev, V. I. 2011b. Hidden oscillations in dynamical systems. Transaction on Systems and Control 6 (2), 54-67.

Leonov, G. A., Kuznetsov, N. V. & Seledzhi, S. M. 2006. Analysis of phase-locked systems with discontinuous characteristics. IFAC Proceedings Volumes (IFAC-PapersOnline) 1, 107-112. doi:10.3182/20060628-3-FR-3903.00021.

Leonov, G. A., Kuznetsov, N. V. & Seledzhi, S. M. 2009. Automation control - Theory and Practice. In-Tech, 89–114. doi:10.5772/7900.

Leonov, G. A., Kuznetsov, N. V. & Seledzhi, S. M. 2011a. Hidden oscillations in dynamical systems. Recent researches in System Science, 292–297.

Leonov, G. A., Kuznetsov, N. V. & Vagaitsev, V. I. 2011b. Localization of hidden Chua's attractors. Physics Letters A 375 (23), 2230–2233. doi:10.1016/j.physleta.2011.04.037.

Leonov, G. A., Kuznetsov, N. V. & Vagaitsev, V. I. 2012. Hidden attractor in smooth Chua systems. Physica D: Nonlinear Phenomena 241 (18), 1482-1486. doi:10.1016/j.physd.2012.05.016.

Leonov, G. A. & Kuznetsov, N. V. 2007. Time-varying linearization and the Perron effects. International Journal of Bifurcation and Chaos 17 (4), 1079-1107. doi:10.1142/S0218127407017732.

Leonov, G. A. & Kuznetsov, N. V. 2010. Limit cycles of quadratic systems with a perturbed weak focus of order 3 and a saddle equilibrium at infinity. Doklady Mathematics 82 (2), 693-696. doi:10.1134/S1064562410050042.

Leonov, G. A. & Kuznetsov, N. V. 2011a. Algorithms for searching for hidden oscillations in the Aizerman and Kalman problems. Doklady Mathematics 84 (1), 475-481. doi:10.1134/S1064562411040120.

Leonov, G. A. & Kuznetsov, N. V. 2011b. Analytical-numerical methods for investigation of hidden oscillations in nonlinear control systems. IFAC Proceedings Volumes (IFAC-PapersOnline) 18 (1), 2494–2505. doi:10.3182/20110828-6-IT-1002.03315.

Leonov, G. A. & Kuznetsov, N. V. 2012. IWCFTA2012 keynote speech I - Hidden attractors in dynamical systems: From hidden oscillation in Hilbert-Kolmogorov, Aizerman and Kalman problems to hidden chaotic attractor in Chua circuits. In Chaos-Fractals Theories and Applications (IWCFTA), 2012 Fifth International Workshop on, XV-XVII. doi:10.1109/IWCFTA.2012.8.

Leonov, G. A. & Kuznetsov, N. V. 2013a. Advances in Intelligent Systems and Computing, Vol. 210 AISC. Springer, 5-13. doi:10.1007/978-3-319-00542-3_3.

Leonov, G. A. & Kuznetsov, N. V. 2013b. Hidden attractors in dynamical systems. From hidden oscillations in Hilbert-Kolmogorov, Aizerman, and Kalman problems to hidden chaotic attractors in Chua circuits. International Journal of Bifurcation and Chaos 23 (1). doi:10.1142/S0218127413300024. (art. no. 1330002).

68

Leonov, G. A. & Kuznetsov, N. V. 2013c. Numerical Methods for Differential Equations, Optimization, and Technological Problems, Computational Methods in Applied Sciences, Volume 27, Part 1. doi:10.1007/978-94-007-5288-7_3.

Leonov, G. A. & Kuznetsov, N. V. 2014, ISBN 978-1-908106-38-4. Nonlinear Mathematical Models Of Phase-Locked Loops. Stability and Oscillations, Vol. 7. Cambridge Scientific Press.

Leonov, G. A., Vagaitsev, V. I. & Kuznetsov, N. V. 2010. Algorithm for localizing Chua attractors based on the harmonic linearization method. Doklady Mathematics 82 (1), 693-696. doi:10.1134/S1064562410040411.

Leonov, G. A. 2006. Phase-locked loops. theory and application. Automation and Remote Control 10, 47–55.

Leonov, G. A. 2008. Computation of phase detector characteristics in phase-locked loops for clock synchronization. Doklady Mathematics 78 (1), 643–645.

Leonov, G. A. 2010. Effective methods for periodic oscillations search in dynamical systems. App. math. & mech. 74 (1), 24-50.

Lin, V., Ghoneim, A. & Dafesh, P. 2004. Implementation of reconfigurable software radio for multiple wireless standards. In Aerospace Conference, 2004. Proceedings. 2004 IEEE, Vol. 2, 1392–1397.

Lindsey, W. & Simon, M. 1973. Telecommunication Systems Engineering. NJ: Prentice Hall.

Lindsey, W. 1972. Synchronization systems in communication and control. New Jersey: Prentice-Hall.

Luo, Z. & Sonkusale, S. 2008. A novel bpsk demodulator for biological implants. Circuits and Systems I: Regular Papers, IEEE Transactions on 55 (6), 1478–1484.

Malyon, D. 1984. Digital fibre transmission using optical homodyne detection. Electronics Letters 20 (7), 281–283.

Manassewitsch, V. 2005. Frequency synthesizers: theory and design. Wiley.

Margaris, W. 2004. Theory of the Non-Linear Analog Phase Locked Loop. New Jersey: Springer Verlag.

Mileant, A. & Hinedi, S. 1994. Overview of arraying techniques for deep space communications. Communications, IEEE Transactions on 42 (234), 1856–1865.

Misra, R. & Palod, S. 2011. Code and carrier tracking loops for gps c/a code. Int. J. Pure Appl. Sci. Technol 6 (1), 1–20.

Mitropolsky, I. A. 1967. Averaging method in non-linear mechanics. International Journal of Non-Linear Mechanics 2 (1), 69–96.

Mitropolsky, Y. & Bogolubov, N. 1961. Asymptotic Methods in the Theory of Non-Linear Oscillations. New York: Gordon and Breach.

Miyazaki, T., Ryu, S., Namihira, Y. & Wakabayashi, H. 1991. Optical costas loop experiment using a novel optical 90 hybrid module and a semiconductor-laser-amplifier external phase adjuster. In Optical Fiber Communication. Optical Society of America, WH6.

Mossaheb, S. 1983. Application of a method of averaging to the study of dithers in non-linear systems. International Journal of Control 38 (3), 557–576.

Nissila, M., Pasupathy, S. & Mammela, A. 2001. An em approach to carrier phase recovery in awgn channel. In Communications, 2001. ICC 2001. IEEE International Conference on, Vol. 7. IEEE, 2199–2203.

Nowsheen, N., Benson, C. & Frater, M. 2010. A high data-rate, software-defined underwater acoustic modem. In OCEANS 2010. IEEE, 1–5.

Proakis, J. G. & Salehi, M. 2007. Digital communications. McGraw-Hill Higher Education.

Razavi, B. 2003. Phase-Locking in High-Performance Systems: From Devices to Architectures.

Roberts, K., O'Sullivan, M., Wu, K.-T., Sun, H., Awadalla, A., Krause, D. J. & Laperle, C. 2009. Performance of dual-polarization QPSK for optical transport systems. Journal of lightwave technology 27 (16), 3546–3559.

Ryan, C. R. & Stilwell, J. H. 1978. QPSK demodulator. (US Patent 4,085,378).

Samoilenko, A. M. 1963. Contribution to the question of the periodic solutions of differential equations with non-differentiable right-hand sides. UMJ XV, 328.

Sanders, J. J. A., Verhulst, F. & Murdock, J. A. 2007. Averaging methods in non-linear dynamical systems, Vol. 59. Springer.

Sarkar, A. & Sengupta, S. 2010. Second-degree digital differentiator-based power system frequency estimation under non-sinusoidal conditions. IET Sci. Meas. Technol. 4 (2), 105–114.

Shah, S. & Sinha, V. 2009. Gmsk demodulator using costas loop for software-defined radio. In Advanced Computer Control, 2009. ICACC'09. International Conference on. IEEE, 757–761.

Shu, K. & Sanchez-Sinencio, E. 2005. CMOS PLL synthesizers: analysis and design. Springer.

Stephens, R. D. 2001. Phase-Locked Loops for Wireless Communications: Digital, Analog and Optical Implementations. Springer.

70

Suarez, A. & Quere, R. 2003. Stability Analysis of Nonlinear Microwave Circuits. New Jersey: Artech House.

Suarez, A., Fernandez, E., Ramirez, F. & Sancho, S. 2012. Stability and bifurcation analysis of self-oscillating quasi-periodic regimes. IEEE transactions on microwave theory and techniques 60 (3), 528–541.

Sutterlin, P. & Downey, W. 1999. A power line communication tutorial - challenges and technologies. In Technical Report. Echelon Corporation.

Tanaka, K., Muto, T., Hori, K., Wakamori, M., Teranishi, K., Takahashi, H., Sawada, M. & Ronning, M. 2001. A high performance gps solution for mobile use. In Proceedings of the 15th International Technical Meeting of the Satellite Division of The Institute of Navigation (ION GPS 2002), 1648–1655.

Tang, X.-M., Xu, P.-C. & Wang, F.-X. 2010. Performance comparison of phase detector in navigation receiver's tracking loop. Journal of National University of Defense Technology 32 (2), 85–90.

Thede, L. 2005. Practical analog and digital filter design. Artech House.

Tomasi, W. 2001. Electronic communications systems: fundamentals through advanced. Pearson/Prentice Hall, 947.

Tomkins, A., Aroca, R. A., Yamamoto, T., Nicolson, S. T., Voinigescu, S. et al. 2009. A zero-IF 60 GHz 65 nm CMOS transceiver with direct BPSK modulation demonstrating up to 6 Gb/s data rates over a 2 m wireless link. Solid-State Circuits, IEEE Journal of 44 (8), 2085–2099.

Tranter, W. H. 2001. Wireless Personal Communications: Bluetooth Tutorial and Other Technologies, Vol. 592. Springer.

Tretter, S. A. 2007. Communication System Design Using DSP Algorithms with Laboratory Experiments for the TMS320C6713TM DSK. Springer.

Troedsson, N. 2009. Method and simulator for generating phase noise in system with phase-locked loop. (US Patent App. 12/371,828).

Vaelimaeki, V., Laakso, T. & Henriksson, J. 1996. Method and circuit arrangement for processing variable symbol rates. (EP Patent 0,741,472).

Valimaki, V., Henriksson, J. & Laakso, T. 1998. Method and circuit arrangement for processing received signal. (US Patent 5,812,608).

Viterbi, A. 1983. Nonlinear estimation of psk-modulated carrier phase with application to burst digital transmission. Information Theory, IEEE Transactions on 29 (4), 543–551.

Wang, L. & Emura, T. 1998. A high-precision positioning servo-controller using non-sinusoidal two-phase type PLL. In UK Mechatronics Forum International Conference. Elsevier Science Ltd, 103–108.

Wang, L. & Emura, T. 2001. Servomechanism using traction drive. JSME International Journal Series C 44 (1), 171–179.

Wang, Y. & Leeb, W. R. 1987. A 90 optical fiber hybrid for optimal signal power utilization. Appl. Opt. 26 (19), 4181–4184. doi:10.1364/AO.26.004181.

Waters, G. W. 1982. Costas loop QPSK demodulator. (US Patent 4,344,178).

Xanthopoulos, T., Bailey, D., Gangwar, A., Gowan, M., Jain, A. & Prewitt, B. 2001. The design and analysis of the clock distribution network for a 1.2 GHz Alpha microprocessor. In Solid-State Circuits Conference, 2001. Digest of Technical Papers. ISSCC. IEEE International, 402–403.

Xu, W., Luo, Z. & Sonkusale, S. 2009. Fully digital bpsk demodulator and multi-level lsk back telemetry for biomedical implant transceivers. Circuits and Systems II: Express Briefs, IEEE Transactions on 56 (9), 714–718.

Young, I., Greason, J. & Wong, K. 1992. A PLL clock generator with 5 to 110 MHz of lock range for microprocessors. Solid-State Circuits, IEEE Journal of 27 (11), 1599–1607.

Young, P. 2004. Electronic communication techniques. Pearson/Prentice Hall, 893.

Yu, G., Xie, X., Zhao, W., Wang, W. & Yan, S. 2011. Impact of phase noise on coherent bpsk homodyne systems in long-haul optical fiber communications. In Photonics and Optoelectronics Meetings 2011. International Society for Optics and Photonics, 83310R–83310R.

Yuldashev, M. V. 2012. Nonlinear Analysis of Costas Loop. Jyväskylä University Printing House. (M.Sc. thesis).

Yuldashev, M. V. 2013a. Nonlinear Mathematical Models of Costas Loops. Saint Petersburg State University Studies in Mathematics.

Yuldashev, R. V. 2013b. Synthesis of Phase-Locked Loop: analytical methods and simulation. Jyväskylä University Printing House. (PhD thesis).